



Calhoun: The NPS Institutional Archive

Theses and Dissertations

Thesis Collection

2005-12

Analysis of the reliability disparity and reliability growth analysis of a combat system using AMSAA extended reliability growth models



Calhoun is a project of the Dudley Knox Library at NPS, furthering the precepts and goals of open government and government transparency. All information contained herein has been approved for release by the NPS Public Affairs Officer.

Dudley Knox Library / Naval Postgraduate School
411 Dyer Road / 1 University Circle
Monterey, California USA 93943

<http://www.nps.edu/library>



NAVAL POSTGRADUATE SCHOOL

MONTEREY, CALIFORNIA

THESIS

**ANALYSIS OF THE RELIABILITY DISPARITY AND
RELIABILITY GROWTH ANALYSIS OF A COMBAT
SYSTEM USING AMSAA EXTENDED RELIABILITY
GROWTH MODELS**

by

Er Kim Hua

December 2005

Thesis Advisors:

Dave Olwell
Morris Driels

Approved for public release; distribution unlimited

THIS PAGE INTENTIONALLY LEFT BLANK

REPORT DOCUMENTATION PAGE			<i>Form Approved OMB No. 0704-0188</i>	
Public reporting burden for this collection of information is estimated to average 1 hour per response, including the time for reviewing instruction, searching existing data sources, gathering and maintaining the data needed, and completing and reviewing the collection of information. Send comments regarding this burden estimate or any other aspect of this collection of information, including suggestions for reducing this burden, to Washington headquarters Services, Directorate for Information Operations and Reports, 1215 Jefferson Davis Highway, Suite 1204, Arlington, VA 22202-4302, and to the Office of Management and Budget, Paperwork Reduction Project (0704-0188) Washington DC 20503.				
1. AGENCY USE ONLY (Leave blank)		2. REPORT DATE December 2005	3. REPORT TYPE AND DATES COVERED Master's Thesis	
4. TITLE AND SUBTITLE: Analysis of the Reliability Disparity and Reliability Growth Analysis of a Combat System using AMSAA Extended Reliability Growth Models.			5. FUNDING NUMBERS	
6. AUTHOR(S) Kim Hua. Er				
7. PERFORMING ORGANIZATION NAME(S) AND ADDRESS(ES) Naval Postgraduate School Monterey, CA 93943-5000			8. PERFORMING ORGANIZATION REPORT NUMBER	
9. SPONSORING /MONITORING AGENCY NAME(S) AND ADDRESS(ES) N/A			10. SPONSORING/MONITORING AGENCY REPORT NUMBER	
11. SUPPLEMENTARY NOTES The views expressed in this thesis are those of the author and do not reflect the official policy or position of the Department of Defense or the U.S. Government.				
12a. DISTRIBUTION / AVAILABILITY STATEMENT Approved for public release; distribution unlimited			12b. DISTRIBUTION CODE	
13. ABSTRACT (maximum 200 words) The first part of this thesis aims to identify and analyze what aspects of the MIL-HDBK-217 prediction model are causing the large variation between prediction and field reliability. The key findings of the literature research suggest that the main reason for the inaccuracy in prediction is because of the constant failure rate assumption used in MIL-HDBK-217 is usually not applicable. Secondly, even if the constant failure rate assumption is applicable, the disparity may still exist in the presence of design and quality related problems in new systems. A possible solution is to apply reliability growth testing (RGT) to new systems during the development phase in an attempt to remove these design deficiencies so that the system's reliability will grow and approach the predicted value. In view of the importance of RGT in minimizing the disparity, this thesis provides a detailed application of the AMSAA Extended Reliability Growth Models to the reliability growth analysis of a combat system. It shows how program managers can analyze test data using commercial software to estimate the system demonstrated reliability and the increased in reliability due to delayed fixes.				
14. SUBJECT TERMS reliability, reliability disparity, reliability testing, RGT, AMSAA Extended Reliability Growth Models.			15. NUMBER OF PAGES 109	
			16. PRICE CODE	
17. SECURITY CLASSIFICATION OF REPORT Unclassified	18. SECURITY CLASSIFICATION OF THIS PAGE Unclassified	19. SECURITY CLASSIFICATION OF ABSTRACT Unclassified	20. LIMITATION OF ABSTRACT UL	

NSN 7540-01-280-5500

Standard Form 298 (Rev. 2-89)
Prescribed by ANSI Std. Z39-18

THIS PAGE INTENTIONALLY LEFT BLANK

Approved for public release; distribution unlimited

**ANALYSIS OF THE RELIABILITY DISPARITY AND RELIABILITY
GROWTH ANALYSIS OF A COMBAT SYSTEM USING AMSAA EXTENDED
RELIABILITY GROWTH MODELS**

Kim Hua Er
Civilian, Defence Science & Technology Agency
B.Eng., Nanyang Technological University, 2000

Submitted in partial fulfillment of the
requirements for the degree of

**MASTER OF SCIENCE IN ENGINEERING SCIENCE
(MECHANICAL ENGINEERING)**

from the

**NAVAL POSTGRADUATE SCHOOL
December 2005**

Author: Kim Hua Er

Approved by: David H. Olwell
Thesis Advisor

Morris R. Driels
Thesis Advisor

Anthony J. Healey
Chairman, Department of Mechanical and Astronautical
Engineering

THIS PAGE INTENTIONALLY LEFT BLANK

ABSTRACT

The first part of this thesis aims to identify and analyze what aspects of the MIL-HDBK-217 prediction model are causing the large variation between prediction and field reliability. The key findings of the literature research suggest that the main reason for the inaccuracy in prediction is because of the constant failure rate assumption used in MIL-HDBK-217 is usually not applicable. Secondly, even if the constant failure rate assumption is applicable, the disparity may still exist in the presence of design and quality related problems in new systems. A possible solution is to apply reliability growth testing (RGT) to new systems during the development phase in an attempt to remove these design deficiencies so that the system's reliability will grow and approach the predicted value. In view of the importance of RGT in minimizing the disparity, this thesis provides a detailed application of the AMSAA Extended Reliability Growth Models to the reliability growth analysis of a combat system. It shows how program managers can analyze test data using commercial software to estimate the system demonstrated reliability and the increased in reliability due to delayed fixes.

THIS PAGE INTENTIONALLY LEFT BLANK

TABLE OF CONTENTS

I.	INTRODUCTION.....	1
A.	BACKGROUND	1
B.	OBJECTIVES AND SCOPE OF RESEARCH	4
C.	POTENTIAL BENEFITS OF RESEARCH	5
II.	ANALYSIS OF THE RELIABILITY DISPARITY.....	7
A.	INTRODUCTION.....	7
B.	KEY CONCEPTS	7
	1. The Bathtub Curve	8
	2. The Exponential Distribution	9
	3. Reliability Prediction Model	10
	a. Parts Count.....	11
	b. Parts Stress.....	11
C.	MAJOR FACTORS AFFECTING RELIABILITY PREDICTION.....	12
	1. Inapplicability of the Constant Failure Rate Assumption in MIL-HDBK-217 Reliability Prediction Model.....	12
	2. Lack of Accurate Failure Rates Data.....	16
	3. Inability to Predict Unexpected Failures Modes Due To Poor Design and Quality Related Problems	16
D.	RECOMMENDATIONS.....	18
III.	RELIABILITY GROWTH PLANNING.....	21
A.	INTRODUCTION.....	21
B.	RELIABILITY GROWTH PROGRAM OF THE COMBAT SYSTEM	22
C.	RELIABILITY GROWTH PLANNING METHODOLOGY.....	23
	1. Development of the Idealized Growth Curve for Subsystem A.....	26
	2. Development of the Idealized Growth Curve for Subsystem B.....	29
IV.	RESULTS AND DISCUSSION OF RELIABILITY GROWTH ANALYSIS.....	33
A.	INTRODUCTION.....	33
B.	AMSAA RELIABILITY GROWTH MODELS.....	33
	1. AMSAA Basic Model for Test-Fix-Test.....	34
	2. AMSAA Projection Model for Test-Find-Test.....	37
	3. Extended Reliability Growth Model for Test-Fix-Find-Test.....	38
C.	RELIABILITY GROWTH ANALYSIS FOR SUBSYSTEM A	40
	1. Phase 1 results and analysis	40
	2. Phase 2 results and analysis	46
	3. Phase 3 results and analysis	50
D.	RELIABILITY GROWTH ANALYSIS FOR SUBSYSTEM B	61
	1. Phase 1 results and analysis	61
	2. Phase 2 results and analysis	67
	3. Phase 3 results and analysis	75

V. CONCLUSIONS	81
LIST OF REFERENCES.....	85
INITIAL DISTRIBUTION LIST	89

LIST OF FIGURES

Figure 1.	The “bathtub” curve [From Ref. 7]	9
Figure 2.	Human hazard rate analysis [From Ref. 11]	14
Figure 3.	Constituent curves of the “bathtub” curve [From Ref. 14]	14
Figure 4.	Failure rate versus time [From Ref. 5]	21
Figure 5.	Example of an idealized growth curve	24
Figure 6.	Idealized growth curve for subsystem A	28
Figure 7.	Idealized growth curve for the subsystem B	31
Figure 8.	MRBF projection for Phase 1	44
Figure 9.	Before and after failure rate for Type BD failure modes in Phase 1 based on frequency and EF	45
Figure 10.	MRBF projection for Phase 2	49
Figure 11.	Failure rate for individual BC failure modes after the test	50
Figure 12.	Cumulative number of failures vs time plot for Phase 3	54
Figure 13.	MRBF vs time plot for Phase 3	55
Figure 14.	Projected MRBF vs time plot for Phase 3	58
Figure 15.	Individual failure rate of Type BC and BD failure modes at the end of Phase 3	59
Figure 16.	MKBF projection for Phase 1	65
Figure 17.	Cumulative number of failures vs time plot for Phase 1	66
Figure 18.	Before and after failure rate for Type BD failure mode in Phase 1	67
Figure 19.	Failure intensity vs time plot for Phase 2	71
Figure 20.	MKBF vs time plot for Phase 2	72
Figure 21.	Failure rate of individual BC failure modes at the end of test	73
Figure 22.	Cumulative number of failures vs time plot for Phase 3	78
Figure 23.	Instantaneous failure intensity vs time plot for Phase 3	79
Figure 24.	MKBF vs time plot for Phase 3	80

THIS PAGE INTENTIONALLY LEFT BLANK

LIST OF TABLES

Table 1.	Ratio disparity between predicted and field MTBF [After Ref. 1]	2
Table 2.	Reliability models/standards [After Ref. 12]	10
Table 3.	Predicted and RDT MTBF [After. Ref. 15]	17
Table 4.	Sensitivity analysis of α on total test duration	27
Table 5.	Summary of test parameters for subsystem A	27
Table 6.	Computed MRBF values for the idealized growth curve	28
Table 7.	Growth rate versus total test duration	29
Table 8.	Summary of test parameters for subsystem B	30
Table 9.	Computed MKBF values for the idealized growth curve	30
Table 10.	Test-find-test data for Phase 1	41
Table 11.	Test-find-test Type B failure mode data and EF for Phase 1	41
Table 12.	RGA 6 PRO projection summary and Cramer Von Mises test results for Phase 1	43
Table 13.	Test-fix-test data for Phase 2	46
Table 14.	Unique first time occurrence BC failure mode for Phase 2	46
Table 15.	RGA 6 PRO analysis summary and Cramer Von Mises test results for Phase 2	48
Table 16.	Test-fix-find-test data for Phase 3	51
Table 17.	Test-find-test Type BD failure mode data and EF for Phase 3	51
Table 18.	RGA 6 PRO failure modes analysis results and Cramer Von Mises statistical test results for Phase 3	53
Table 19.	RGA 6 PRO BD failure modes analysis results and Cramer Von Mises statistical test results for Phase 3	57
Table 20.	Test-find-test data for Phase 1	61
Table 21.	Test-find-test Type B failure mode data and effectiveness factor for Phase 1	62
Table 22.	RGA 6 PRO projection summary and Cramer Von Mises test results for Phase 1	64
Table 23.	Test-fix-test data for Phase 2	68
Table 24.	Unique first time occurrence BC failure mode for Phase 2	68
Table 25.	RGA 6 PRO analysis summary and Cramer Von Mises test results for Phase 2	70
Table 26.	Test-fix-test data for Phase 3	75
Table 27.	RGA 6 PRO analysis summary and Cramer Von Mises test results for Phase 3	77

THIS PAGE INTENTIONALLY LEFT BLANK

ACKNOWLEDGMENTS

The author would like to thank his thesis advisors, Professor David H. Olwell, and Professor Morris Driels for their guidance during the research and analysis phase of this study. Their insights and expert knowledge on the subject of reliability were invaluable to this study. Additionally, the author is grateful to Chee Kong for his help in this thesis. Finally, the author would also like to thank ReliaSoft Corporation for offering a free evaluation copy of the RGA 6 PRO software that has made this study possible.

THIS PAGE INTENTIONALLY LEFT BLANK

EXECUTIVE SUMMARY

One of the major problems in today's military systems is the issue of poor reliability, and the inconsistency between predicted and field reliability. Experience has shown that two reasons are: 1) the inability to consistently predict field reliability using reliability prediction models, and 2) inadequate emphasis on reliability testing prior to system fielding, as more emphasis is being placed on meeting performance requirements than reliability requirements. The first part of this thesis aims to identify and analyze what principal aspects of the MIL-HDBK-217 prediction model are causing the large variation between prediction and field reliability with the ultimate goal of minimizing the gap. The second part of the thesis demonstrates how the Duane reliability growth model can be used as a useful tool for the purpose of reliability growth planning and also to apply the AMSAA Extended Reliability Growth Models for analyzing reliability growth.

The key findings of the literature research suggest that the main issues are some of the inherent assumptions of the MIL-HDBK-217 prediction model. First, the constant failure rate assumption that has been generally applied in reliability prediction is usually not applicable. However, Drenick's theorem has proven that complex repairable systems, under certain constraints, can be well represented by the exponential distribution. The reliability engineer must be able to recognize when the mathematical simplicity of the constant failure rate model can be used without a substantial penalty in prediction accuracy. Secondly, the lack of accurate failure rates data is also another reason because the task of acquiring field data of components is very time consuming. A well designed part is less likely to fail early, leading to extended waiting time for any useful information. A possible solution is to apply accelerated life testing to components to shorten the waiting time required for acquiring failure rates data. Lastly, even if the exponential distribution is applicable, the disparity between predicted and field reliability may still exist in new systems because of unexpected failure modes that may arise in the presence of design and quality deficiencies which will prevent the system from reaching the predicted value. A possible solution is to apply reliability growth testing (RGT) to

new systems during the development phase in an attempt to remove these design deficiencies so that the system's reliability will grow and approach the predicted value. In contrast to the MIL-HDBK-217 prediction model, AMSAA reliability growth models assume that system failures during development follow a Non-Homogeneous Poisson Process (NHPP).

In view of the importance of RGT in minimizing the disparity, this thesis provides a detailed application of the AMSAA Extended Reliability Growth Models to the reliability growth analysis of a combat system. It shows how program managers can analyze test data using commercial software to estimate the system's demonstrated reliability and the increased in reliability due to delayed fixes. The example combat system consists of two main subsystems. The reliability growth for both the subsystems is tracked over three phases of testing. Reliability is tracked on a phase by phase basis using test data collected within each test phase. The type of reliability growth model selected for is based on the type of management approach employed in each test phase. The three types of AMSAA reliability growth models are: 1) AMSAA Extended Model for Test-Fix-Test, 2) AMSAA Extended Test-Find-Test Projection Model, and 3) AMSAA Extended Model for Test-Fix-Find-Test.

The results of the reliability analysis for the combat system show that the demonstrated system reliability for both subsystems is initially low but improves as testing progresses. Reliability is finally estimated to meet the predicted value as failure modes are discovered and eliminated through the Test-Analyze-And-Fix (TAAF) process towards the target reliability by application of the TAAF approach. I conclude that the application of RGT during the developmental phase is effective in minimizing the disparity between predicted and field reliability. Systems that bypass development testing will experience low reliability in the field, which is one of the main causes of disparity between predicted and field reliability.

There are also some important lessons learned on the use of the reliability growth models from this thesis. For the Duane's Model, the total test time required for an RGT program is sensitive to the system's initial reliability, initial test time, and growth rate. In

most practical cases, the total test time is usually fixed due to time and resources available in the development program

The use of failure mode designation in AMSAA Extended Reliability Growth Models has proven to be beneficial as it can provide many useful metrics in reliability growth analysis and for decision making during the test program. They are: 1) initial system reliability at the beginning of a test phase, 2) the average effectiveness factor (EF) of remedying failure modes, 3) fraction of seen and unseen Type BD failure modes, and 4) system failure rate breakdown for individual failure modes. Knowing the failure rate breakdown of individual failure modes in the system is important as it enables easy identification of failure modes with relatively high failure rate. It is also important to note that the final system reliability is sensitive to the assigned value of EF for Type BD failure modes. To prevent over estimation of the system final reliability, a conservative EF should be assigned since the actual effectiveness of the delayed fixes cannot be determined without further testing.

For new systems under development, the use of the AMSAA NHPP model provides a better representation of the system's failure rate than the exponential distribution because the failure rate is varying with time as testing progresses. Once the system matures through a period of testing and reliability growth has reached a plateau, the system's failure rate will tend towards being well represented by an exponential distribution.

THIS PAGE INTENTIONALLY LEFT BLANK

I. INTRODUCTION

A. BACKGROUND

Reliable weapon systems are critical elements for fighting and winning wars, and reliability is an effective force multiplier that contributes towards higher operational readiness and a reduced logistics footprint. One of the major problems in today's military systems is the issue of poor reliability, and the inconsistency between predicted and field reliability. Experience has shown that two reasons for this inconsistency are: 1) the inability to consistently predict field reliability using reliability prediction models, and 2) inadequate emphasis on reliability testing prior to system fielding as more emphasis is being placed on meeting performance requirements than reliability requirements [Ref. 1 and Ref. 2].

This chapter first introduces the issues concerning the inability to predict field reliability, the importance of reliability testing for military systems, and follows by introducing the concept of reliability growth. The scope and objectives of this research are then presented along with the potential benefits.

Within the military, there is a need in the early stages of the development program to accurately predict the expected field reliability of military systems for logistics and operational planning purposes. These include the determination of spares quantity, forecast of maintenance support cost, life cycle cost, and systems availability analysis. These analyses require accurate reliability predictions. Research has shown, however, that the field reliability of weapon systems has often failed to measure up to its predicted Mean-Time-Between-Failure (MTBF) [Ref. 1].

Empirically it has been found that the ratio of the predicted MTBF to its field MTBF for military systems can vary by as much as 20:1 [Ref. 1]. Table 1 presents some examples of this disparity.

Equipment	Reliability Ratio Predicted: Field
Airborne Avionics	>20:1
Airborne Radar	5.0:1
Airborne Fighter	9.1:1
Airborne Transport	2.3:1

Table 1. Ratio disparity between predicted and field MTBF [After Ref. 1]

Reliability prediction is performed during the early design phase, when the prototype is not yet built, to estimate the expected field reliability of the system. The most widely used prediction method in the military is the MIL-HDBK-217. Although DoD has discontinued updates of MIL-HDBK-217F, this standard is still widely used in the military. Its effectiveness has not been clearly established since it has been shown that there exist large variations between predicted and field reliability. Research efforts are required to examine the problems of the MIL-HDBK-217 prediction model that have caused this disparity.

The inability to relate predicted reliability to field reliability could have severe impact from both the logistics and operational perspective. A recent analysis performed on the Comanche helicopter by an NPS student indicates that missing the predicted availability by just one percent could increase the life-cycle Operation & Support (O&S) cost by more than \$75 million [Ref. 3].

As important as reliability prediction is, its value starts to diminish once prototypes are built and the reliability can be assessed via testing. Reliability prediction and reliability testing play different roles but they complement one another at different

stages of the product development cycle. Reliability testing is performed to ensure that the fielded system meets the specified level of reliability.

Over the years, there were numerous reported cases of military systems exhibiting poor reliability. One example is the Hunter Unmanned Aerial Vehicle (UAV) System [Ref. 4]. The urgent need for the US Army to have a UAV System forced the Hunter System to be fielded without going through its development phase which means that the system was not adequately tested. Consequently, several Air Vehicles (AVs) were lost due to various failures and that finally resulted in a decision to terminate the production program. The lesson learned is to recognize the significance of reliability testing during the development phase. Reliability can only be validated with rigorous testing under actual combat conditions. This is especially important for complex and state-of-the-art weapon systems. There are too many uncertainties and risks involved, especially in the area of systems design, and it is virtually impossible for designers to predict in advance all possible sources of failure modes. Failure to achieve an acceptable level of reliability at this late stage of development can have a devastating impact on the program, including fielding a less reliable weapon system and incurring additional cost for retesting and redesign.

Reliability testing does not guarantee that reliability targets will be met ultimately but having a strong emphasis on reliability testing should substantially increase the chances of meeting these objectives. During system development, the eventual goal for the system's reliability is known as the reliability target. However, the initial prototypes produced will almost certainly contain design, quality, and other engineering related flaws that prevent a prototype from reaching the target immediately. In order to improve the reliability, the prototypes are subjected to intensive testing to identify and implement corrective actions to improve the design. This process of testing, fixing, and testing to increase the system's reliability is known as reliability growth. Reliability growth is generally quantified by an increase in mean time between failures over time. The intervals between failures will become longer on average if there is positive reliability growth. On the other hand, if negative growth is occurring, these intervals will tend to be shorter. For no growth, the intervals will retain the same mean.

The estimation of system reliability involves the use of a reliability growth model. A reliability growth model is an analytical model that represents the reliability of the system during the development process. It accounts for the changes in reliability due to all corrective actions incorporated during the developmental phase. The basic principle of a reliability model is to apply the failure data collected during prototype testing to determine the reliability of the system. A reliability model is also used for developing a test plan to determine the amount of test time required to meet the reliability targets. Once the test plan is developed, the model can be used as data is collected to estimate the reliability of the system during the test phase in order to know how much additional testing is required to meet the target. Extrapolating a growth curve beyond the current data estimates what reliability a program can be expected to achieve providing that the conditions of the test and the engineering effort to improve reliability are maintained at their present levels.

Although many models existed for modeling reliability growth, the Duane and the US Army Materiel Systems Analysis Activity (AMSAA) models are among the most widely used in the military [Ref. 5]. The deterministic nature of the Duane's model is commonly used for constructing the idealized growth curve in reliability growth planning. The AMSAA model employs the Weibull process to model reliability growth and its statistical nature allows estimation of unknown parameters using test data which makes it a useful tool for reliability assessment.

B. OBJECTIVES AND SCOPE OF RESEARCH

The first part of this thesis aims to identify and analyze what principal aspects of the MIL-HDBK-217 prediction model are causing the large variation between prediction and field reliability.

The second part of the thesis aims to demonstrate the use of the Test-Analyze-And-Fix (TAAF) concept for the reliability growth analysis of a combat system. The main intent is to demonstrate how the Duane reliability growth model can be used as a

useful tool to construct an idealized growth curve for the purpose of reliability growth planning and also to apply the AMSAA Extended Reliability Growth Models for analyzing reliability growth.

Lastly, lessons learned and recommendations on reliability growth based on this research will be presented in this thesis.

C. POTENTIAL BENEFITS OF RESEARCH

This research consolidates some important findings that has given rise to the inaccuracy in the MIL-HDBK-217 reliability prediction with the ultimate goal of minimizing the gap between predicted and field reliability.

This thesis also shows how program managers can plan and analyze test data using commercial software to estimate the system's demonstrated reliability and estimate the increased in reliability due to delayed fixes.

THIS PAGE INTENTIONALLY LEFT BLANK

II. ANALYSIS OF THE RELIABILITY DISPARITY

A. INTRODUCTION

Within the military, accurate prediction of system reliability plays a critical role from both the logistics and operational perspective. MTBF figures are used for many logistics and operational planning activities [Ref. 6]. They include the following:

Spares Provisioning. Determination of spare quantities purchased to meet operational availability. Components with higher failure rates needs to be stocked at a higher number.

Development of Maintenance Strategies. In many cases, MTBF is used to determine the preventive maintenance intervals of a component.

Estimation of Life Cycle Cost. Estimation of the total system cost on a yearly basis.

Unfortunately, there are a host of factors that give rise to the disparity between predicted and field MTBF. The focus here is to identify and analyze principal aspects of the MIL-HDBK-217 prediction model that are causing the large variation between prediction and field reliability.

The remaining of this chapter will first discuss the key concepts pertinent to the understanding of the research theme which include the “bathtub” curve, the exponential distribution, and the principles of reliability prediction and follow by a discussion on the results, conclusions and recommendations.

B. KEY CONCEPTS

This section provides a fundamental understanding of the key concepts related to reliability prediction such as the “bathtub” curve, the exponential distribution and also the principles of reliability prediction in order to understand the research theme--the reliability disparity.

1. The Bathtub Curve

Figure 1 shows a “bathtub” curve that is often used in the field of reliability to describe the failure rate behavior of a system over its life cycle. The vertical axis of the “bathtub” curve represents the hazard rate or the instantaneous failure rate. The hazard rate applies only to non repairable systems in which only one failure can occur. For repairable systems the term failure rate or rate of occurrence of failure is more appropriate. The “bathtub” curve consists of three distinct regions: infant mortality, useful life and wear-out [Ref. 7].

The infant mortality region exhibits a decreasing failure rate, characterized by early failures attributable to defects in design, manufacturing or construction. The failure rate decreases with time as the design defects are detected and repaired. The failure rate is the probability of failure in the next interval of time given that an item has survived to a certain age, divided by the length of the interval. It is an important function in reliability analysis since it shows changes in probability of failure over the lifetime of a system. One way to eliminate such failures is through design and production quality control measures that will reduce variability and hence infant mortality failures [Ref. 12].

The useful life region by assumption has a reasonably constant failure rate, characterized by random failures. These failures are likely caused by unavoidable load rather than any inherent defect in the system. There are many forms of possible external loadings such as temperature fluctuations, vibration, power surges and moisture variation. Random failures can be reduced by increasing the robustness of the design and/or controlling the external environment.

The wear-out region has an increasing failure rate characterized by the aging phenomena. The typical failure mechanisms are corrosion, fatigue cracking, embrittlement, and diffusion of materials.

In reliability prediction, the failure rate of a system has often been assumed to be constant which resembles the useful life region of the bathtub curve as shown in Figure 1. In reality, the assumption of constant failure rate is more representative of an electronic

system rather than a mechanical system. Failure occurrences in electronic systems are considered as random and are assumed to follow a Poisson process.

On the other hand, the failure distribution of mechanical hardware is characterized by an initial wear-in period and followed by a long span of increasing failure rate. The primary failure mechanisms for mechanical systems are corrosion, fatigue and other cumulative effects.

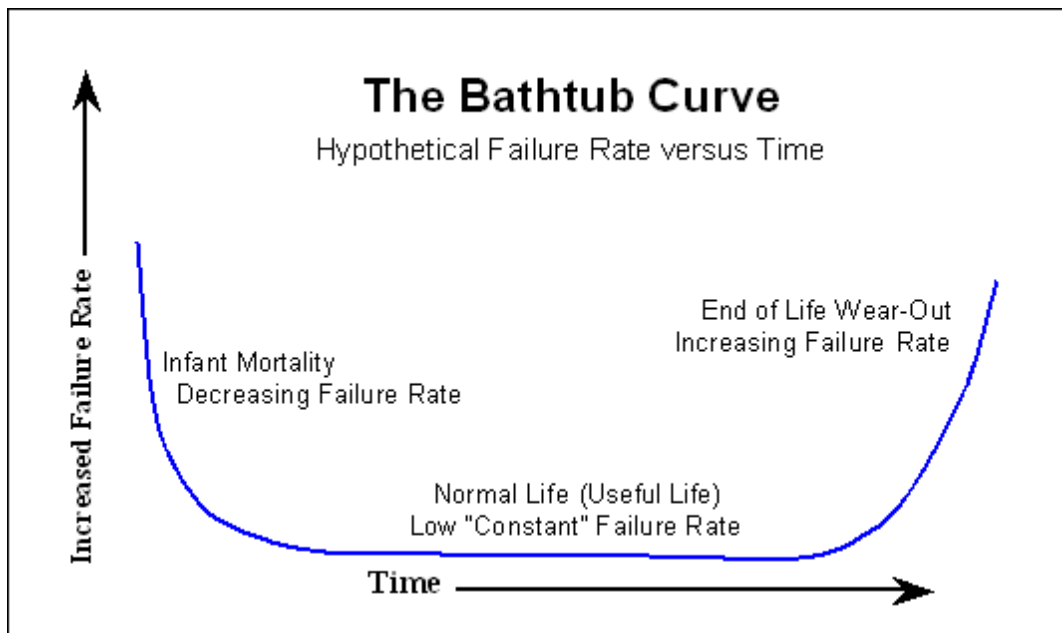


Figure 1. The “bathtub” curve [From Ref. 7]

2. The Exponential Distribution

The exponential distribution models the failure rate in the useful life region of the bathtub curve as it assumes that the rate at which the system fails is independent of its cumulative age [Ref. 8]. This assumption greatly simplifies the mathematics involved in reliability analysis as it is much easier to calculate with an assumed constant failure rate than to derive the parameters of a two-parameter distribution (e.g., Weibull). This is one of the main reasons for its wide application in many reliability analyses.

Further, it is the lack of memory property of the exponential distribution that assumes a repaired system is as good as new. For the exponential distribution, reliability as a function of time and failure rate, λ , is written as

$$R(t) = e^{-\lambda t}. \quad (2.1)$$

3. Reliability Prediction Model

MIL-HDBK-217, the Military Handbook for “Reliability Prediction of Electronic Component” is the standard reference used in the military for reliability prediction of electronic equipment parts. It was published by the Department of Defense (DoD) in the 1960s. Since then it has been updated several times, with the most recent Revision F Notice 2, released in February 1995 [Ref. 9]. Table 2 shows some of the prediction models available in the military and commercial industry.

Model	Description
MIL-HDBK-217	Original worldwide standard (MIL-STD-217) for commercial & military electronic components
Telcordia SR-332	Original Bellcore standard for commercial grade electronic components
PRISM	Originally developed by the Reliability Analysis Center (RAC), incorporates process grading factors
CNET 93	Developed by France Telecom

Table 2. Reliability models/standards [After Ref. 12]

Conventional reliability prediction assumes that all failures are independent. It first defines the failure rate of all the key components that made up the system and sums them up to obtain the overall system failure rate, assuming a series system. The MIL-HDBK-217 reliability prediction model assumes a constant failure rate for all the components. The validity and usefulness of this assumption has often been challenged by practitioners in the field of reliability. Many have denounced the use of this assumption

as not being practical as it assumes that a system does not wear out over time. MIL-HDBK-217 consists of two approaches: Parts-Count and Parts-Stress.

a. Parts Count

Parts-Count approach is simpler as it requires less information than the Parts-Stress approach. It only requires knowledge of the quantities of components, application environment and quality factor, π_Q . A quality factor that is above 1.0 implies a poor quality component. The prediction for each part is governed by the application of a quality factor to a base failure rate. The quality factor for most standard electronic components can be found in MIL-HDBK-217. This approach is most useful in the early design stage when the system hardware is not yet available.

MIL-STD-217F parts count defines the overall equipment failure rate as:

$$\lambda_{EQUIP} = \sum_{i=1}^n N_i (\lambda_g \pi_Q)_i \quad (2.2)$$

λ_g = Failure rate of the i^{th} generic part

n = Number of generic part categories

N_i = Quantity of the i^{th} generic part

π_Q = Quality factor of the of the i^{th} generic part

b. Parts Stress

The Parts-Stress approach is more complex as it takes into account the various stress factors such as temperature, environment, quality, electrical, etc, on the component. The electrical stress is usually defined as a ratio of the operating value to the rated value. For instance, the defining stress factor for a resistor is current. Therefore, the operating current and rated current are used in the part stress calculation model. This approach is more applicable later in the design phase when the hardware and knowledge of the operating environment are available in order to estimate the various stress factors.

The models for the MIL-HDBK-217 Parts-Stress approach is much more detailed and varied across part types. The model for the low frequency diode is shown below [Ref. 17].

$$\lambda_p = \lambda_b \pi_T \pi_S \pi_Q \pi_E \quad (2.3)$$

λ_p = Part failure rate

λ_b = Base failure rate

π_T = Temperature factor

π_E = Environment factor

π_Q = Quality factor

π_S = Electrical stress factor

The accuracy of both approaches is highly dependent upon the availability and accuracy of data such as the base failure rate and the various required factors.

C. MAJOR FACTORS AFFECTING RELIABILITY PREDICTION

There are a number of studies that either directly or indirectly address the problem of the reliability disparity. This section focuses on the limitations of the MIL-HDBK-217 model. The key findings of the literature research suggest that the disparity stems from some inherent assumptions of the MIL-HDBK-217 model. For example, the constant failure rate assumption that has been generally applied in reliability prediction is usually not applicable. The lack of accurate field failure rates of components or parts can also affect prediction accuracy. Further, the prediction model cannot predict unexpected failure modes that occur in the field due to poor design and poor quality control.

1. Inapplicability of the Constant Failure Rate Assumption in MIL-HDBK-217 Reliability Prediction Model

System failures can be assumed to follow a Poisson process if the times to failure of all the components that make up a system can be regarded as exponential and component failures to be independent. The rate of failure occurrence of the system can

then be obtained by summing up the failure rates of the individual components. This has been regarded as reasonable for electronic components, and thus provides the basis for MIL-HDBK-217 prediction model. The exponential distribution also assumes all repairs, no matter how minor, restore the system to an “as new” condition. This assumption is often in strict contrast to reality for the following reasons [Ref. 10]:

1. Failure and repair of one part may cause damage to other parts. Therefore, the times between successive failures are not necessarily independent.

2. Repairs may not totally renew the system. Repairs can be imperfect or they introduce other defects leading to failures of other parts. The lack of memory property of the exponential distribution might not be valid in every case.

Since component failures are not always independent, the principle of summing up the failure rates of the individual components to obtain the overall system’s failure rate might not result in the best estimate.

Below are two examples to further describe the limitations of using the constant failure rate assumption of the exponential distribution for reliability prediction.

Figure 2 shows the results of using the exponential and Weibull distributions to model the human mortality rate [Ref. 11]. Similarly, the failure rate distribution is also representative of a system with a short period of useful life follows by a long period of wear-out. It can clearly be seen from Figure 2 that the exponential distribution has grossly under-estimated the later failure rate while over-estimating the initial failure rate. In contrast, the Weibull distribution is more suitable in such a situation. The purpose of this example is to show that the constant failure rate assumption does not apply to a system with a dominant wear-out failure mechanism.

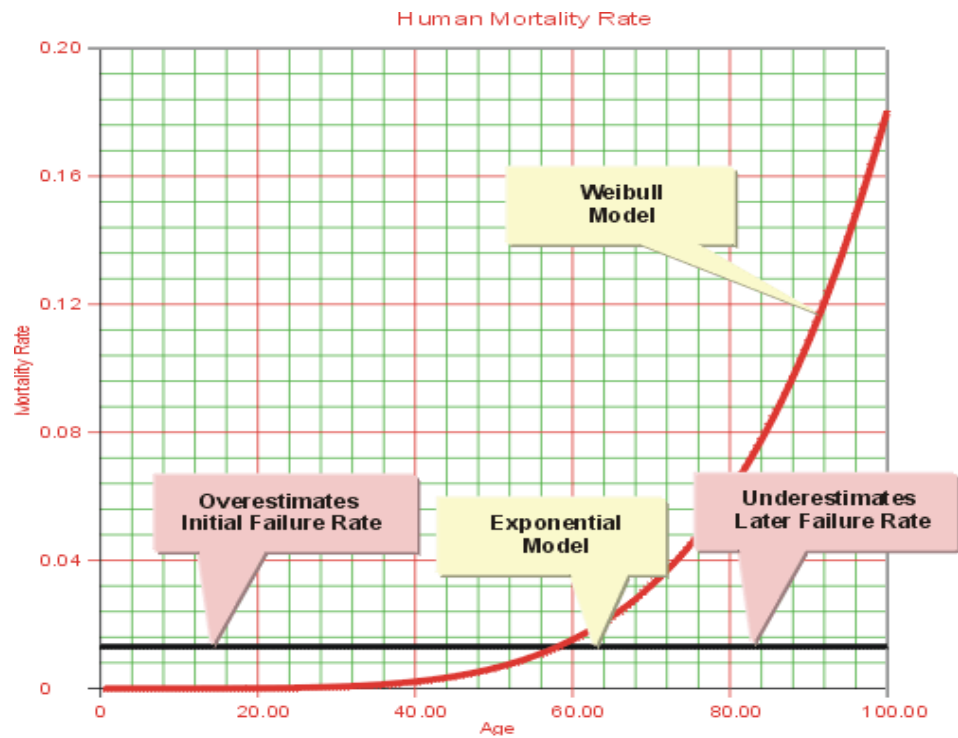


Figure 2. Human hazard rate analysis [From Ref. 11]

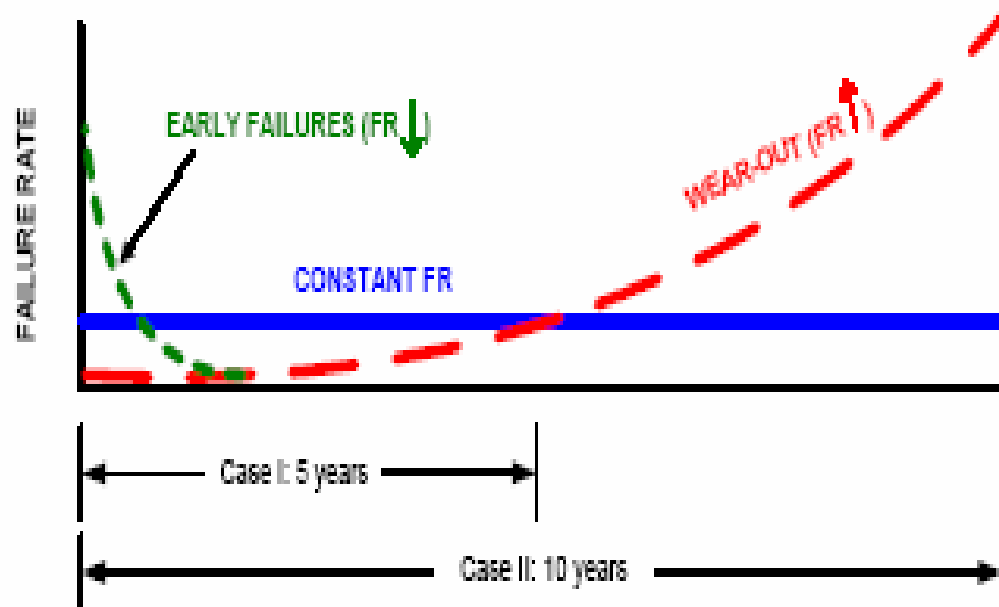


Figure 3. Constituent curves of the "bathtub" curve [From Ref. 14]

Further, the applicability of the constant failure rate assumption also hinges strongly upon the relationship between the system's nature and its life cycle [Ref. 14]. Figure 3 shows a typical bathtub curve with the three distinct regions. The failure rate of an electronic equipment with a maximum of life cycle of five years can be approximated by Case I. Case II approximates a mechanical equipment with a life cycle of ten years. In comparison between the two cases, the results indicate that the constant failure rate assumption has provided a better approximation for a five year period. The reliability is given by the following equation.

$$R(t) = e^{-H(t)} \quad (2.4)$$

$H(t)$ = Cumulative hazard rate

The failure rate was first under-estimated during the early failure region and then over-estimated during the constant failure rate region. Overall, it still provides a fairly good approximation.

On the other hand, the error between prediction and actual is simply too great for a ten year period due to the relatively long period of increasing failure rate in the wear-out region. This brings to an important conclusion that the use of the constant failure rate assumption is highly dependent upon the system's life cycle.

In addition, a similar conclusion that can be drawn from the two previous examples is that the constant failure rate assumption tends to produce a conservative estimate of the system's overall failure rate that is dependent upon the relative period of wear-out region over its life cycle. As observed from Figure 3, the wider the wear-out region over the life cycle, the greater will be the error margin. This further reinforces the point that it is not suitable for predicting failure rates of a system with a dominant wear-out failure mechanism. Reliability prediction using this assumption for a system characterized by a long period of wear-out provides little insights from the logistics planning perspective as it can result in severe spares under-purchased. All these reasons explain why reliability prediction using the constant failure rate assumption often yields inconsistent results from field reliability.

2. Lack of Accurate Failure Rates Data

A reliability prediction model is effectively a set of “best guesses” and to achieve any degree of accuracy they must use empirically acquired field data. Prediction accuracy to a large extent depends on the amount of field data available and the painful fact is that data collection takes a long time [Ref. 13].

The task of acquiring field data of components is not a simple task because it takes time for a component to fail before meaningful data on failure rates can be gathered. A well designed part is less likely to fail early, leading to extended waiting time for any useful information. Because the task is so time consuming, there are relatively few sources, usually from the manufacturers themselves. The largest sources of field data are the Non-electronic Parts Reliability Data (NPRD-95) and Electronic Parts Reliability Data (EPRD-97) produced by the military [Ref. 18]. These were compiled through years of observation, repair records, and other activities. Since failure rate depends mainly on design and application, these data are not representative of all cases. Further, the rapid development of electronic technology limits the ability to collect ample data for any particular technology.

A possible solution to shorten the waiting time for acquiring failure rates data is to apply accelerated life testing (ALT) to components. Accelerated life testing are component life tests with components operated at high stress and failure data observed [Ref. 22].

3. Inability to Predict Unexpected Failures Modes Due To Poor Design and Quality Related Problems

Westinghouse Defense and Electronic Center performed a case study on a complex Electric Countermeasures (ECM) military radar system that underwent a

Reliability Demonstration Test (RDT) to study the differences between predicted and field reliability and analyzed these problems in light of the MIL-HDBK-217 prediction model [Ref. 15].

	Predicted MTBF	RDT MTBF
Radar System	282 hours	100 hours

Table 3. Predicted and RDT MTBF [After. Ref. 15]

It was found that the main differences are related to the assumptions made of the quality of design and the adherence to the established and specified quality control procedures in producing the parts. The MIL-HDBK-217 model inherently assumes that certain standards are followed in these areas based on specified engineering requirements but this assumption is not always valid in all cases. Two examples of failures that were identified during the RDT test will be presented to support this claim.

The first failure to be discussed is due to a design deficiency of a thin film RF amplifier. This failure arises because of inadequate clearance between the toroid of the RF amplifier and the lid case that was not foreseen during the initial design of the device. The toroid was being mounted too closely to the device lid and that subsequently resulted in a short circuit due to contact with the lid of the case after several cycles of thermal cycling that caused the toroid to move relative to its original position. The assumption during the initial reliability prediction of this device was that all design considerations for this device were completely satisfied. Obviously, these assumptions were not valid for this case.

The second failure concerns thick film devices that consists of many discrete parts and solder joints. Solder balls form as a result of the solder flow process being out of control, in that the solder flow temperature deviated from the specified range during the device manufacturing process. The resulting solder balls, which were loosely attached at various points of the device, broke loose and lodged between various chips and substrate causing component to substrate short circuit. Reliability prediction is unable to predict

these unexpected failure modes that arise as a result of poor quality control as it inherently assumes that all processes are in proper control.

The two failures previously described were a direct result of poor design and lack of quality control, respectively, which were identified during RDT. During the initial reliability prediction prior to production and test, it is almost impossible to know in advance how good these control methods and engineering designs would be. Therefore it is extremely important to be aware of the differences between the inherent assumptions of the MIL-HDBK-217 prediction model and the many uncertainties that can happen during the actual engineering process.

D. RECOMMENDATIONS

The constant failure rate model is mathematically simple for reliability prediction but it is not always applicable. It serves as a good approximation for a system that is characterized by a long period of useful life and a short period of early failure. In order to improve the precision of reliability prediction, the reliability engineer must be able to recognize when the mathematical simplicity of the constant failure rate model can be used without a substantial penalty in prediction accuracy. This can be achieved by analyzing the failure rate distribution of a system over its intended life and deciding if the exponential distribution is applicable. The failure rate distribution of a system can be estimated by analyzing the failure trends of similar class of systems.

It is also important to be aware of Drenick's Theorem that has proven that complex repairable systems, under certain constraints, tend towards being well represented by the exponential distribution [Ref. 18]. Given that most military systems (aircraft, artillery guns, or naval ships) are usually composed of a large number of components, it would seem that the constant failure rate assumption is applicable. The usefulness of Drenick's Theorem depends on the following constraints. These constraints are: 1) the subcomponents must be in series. 2) The subcomponents fail independently. 3) A failed component is replaced immediately. 4) The replaced subcomponent must be identical. 5) A few system repairs have already been made. Once these conditions are met

and as the number of subcomponents increases, system failures will tend to be exponentially distributed regardless of the failure distributions of the subcomponents. This proof allows reliability practitioners to disregard the failure distribution of the individual components that make up the system since the overall system will fail exponentially

However, one must be aware that using the constant failure rate assumption has the tendency to produce a conservative estimate of the overall system failure rate and this is important from the logistics perspective especially in the purchase of spares. Alternatively, the Weibull distribution provides a possibly more accurate prediction but it will increase the mathematical complexity. There is always a tradeoff between accuracy and mathematical complexity.

Even if the exponential distribution can be used to model a system, the disparity between predicted and field reliability may still exist in new systems because of unexpected failure modes that may arise in the presence of design and quality deficiencies which will prevent the system from reaching the predicted value. One possible solution to eliminate or reduce the frequency of occurrence of unexpected failures in the field is to apply reliability growth testing (RGT) during the development phase. In contrast to the exponential distribution, AMSAA reliability growth models used for reliability growth analysis assume that system failure rate follows a Non Homogeneous Poisson Process (NHPP). Reliability growth testing recognizes that the drawing board design of a complex product cannot be perfect from the reliability point of view and allocates necessary time and resources to fine tune the design by finding those problems that are impossible to know in advance during reliability prediction and designing them out. It follows the formal process of Test-Analyze-And-Fix (TAAF) which involves testing the system to surface all possible failure modes, analyzing the underlying failure mechanism to determine its root causes, implementing corrective actions to improve the design and finally re-testing to verify the effectiveness of the corrective actions to prevent future occurrences. Once the system matures through a period of testing and reliability growth has reached a plateau, the system's failure rate will tends towards well represented by an exponential distribution. Consequently, the disparity between predicted and field MTBF can be minimized. It is also important to

realize that in order to maximize the benefits of a reliability growth program, it has to be conducted as early as possible in the development phase once the prototype is available. The earlier these problems are identified, the better it is so that more time will be available to verify the effectiveness of the design changes. Furthermore, the cost associated with redesigning a product late in the development cycle is extremely high.

The remaining chapters of this thesis will discuss the reliability growth testing of a 155mm SPH artillery gun using reliability growth methodology. The next chapter first introduces the reliability growth methodology and follows by illustrating the use of the Duane's model to determine the essential parameters needed for constructing the idealized growth curve as part of reliability growth planning.

III. RELIABILITY GROWTH PLANNING

A. INTRODUCTION

Reliability growth is the improvement of a product's reliability over time (hence the term growth) using the TAAF philosophy through learning about the deficiencies of the design and taking action to eliminate or minimize the effect of these deficiencies. The growth in reliability is quantified by a decrease in system's failure rate or increase in the test phase average MTBF over time due to the removal of failure sources. Figure 4 reflects a decreasing trend in failure rate which signifies reliability improvement over time.

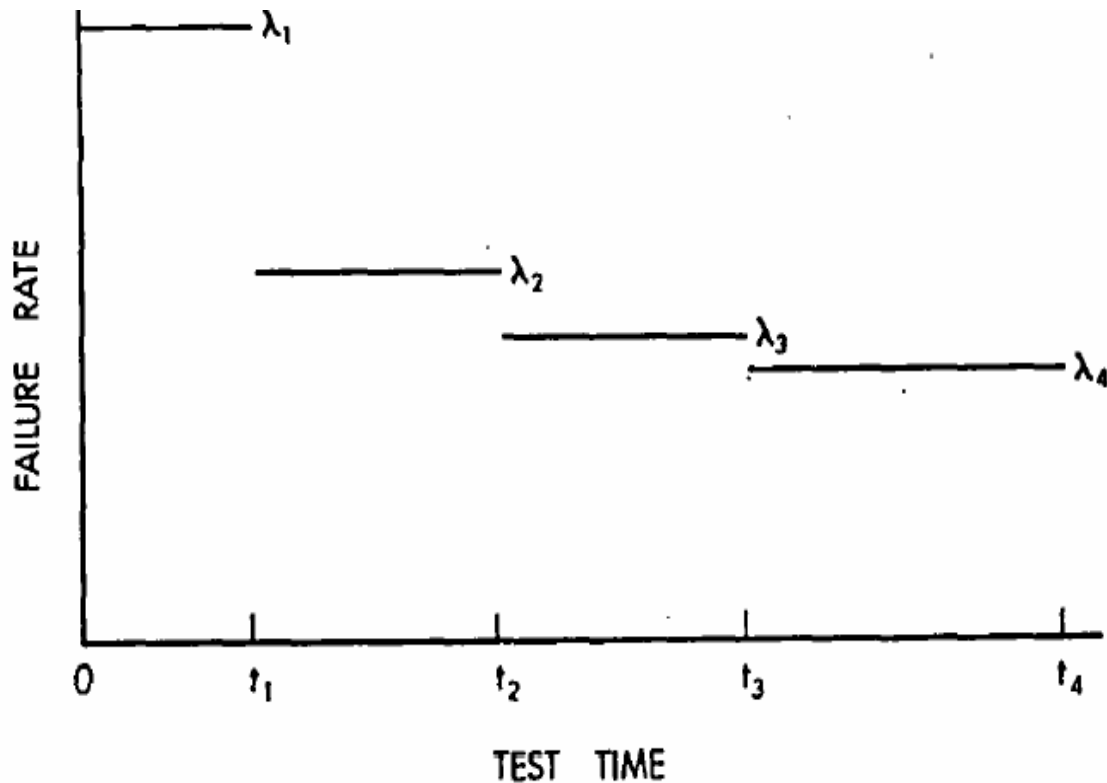


Figure 4. Failure rate versus time [From Ref. 5]

The success of a reliability growth program is dependent on factors including the initial planning of the reliability program and an accurate assessment of the system's current reliability status. It is important to track reliability throughout the test program.

This is accomplished by assessment of system reliability at the end of each test phase and comparing the current reliability and the planned reliability. Planning and tracking of reliability growth requires the use of mathematical models.

One mathematical model used for developing an idealized growth curve in reliability growth planning is Duane's model. A second mathematical model used for tracking reliability growth is the Non-Homogeneous-Poisson-Process (NHPP) model known as the AMSAA model [Ref. 16]. In contrast to the constant failure rate model used in reliability prediction, the AMSAA model describes the failure rate of the system as a function of time.

B. RELIABILITY GROWTH PROGRAM OF THE COMBAT SYSTEM

The development of a large combat system generally involves years of design, testing, fault diagnosis, and redesign to assure that when the system development is completed, the final system meets or exceeds the user requirements. Reliability Growth Testing (RGT) was implemented on one unit of the prototype as part of the Reliability and Maintainability (R&M) program. The combat system consists of two major subsystems which are known as subsystem A and B. The ultimate goal of the combat system reliability growth testing program is to achieve the stated reliability requirements for both subsystems.

The reliability growth program for the combat system focuses on the following areas:

- Reliability growth planning: To develop an achievable solution based on available resources and schedule constraints.
- Test-Analysis-And-Fix (TAAF): Failure causes are isolated, analyzed and then fixed.
- Reliability growth tracking: To determine if reliability requirements have been demonstrated.

The RGT is to subject a single unit of prototype under actual field conditions. All the failures that were surfaced during the test were analyzed and fixed and re-tested. As the testing progresses, these fixes are incorporated into the prototype so that reliability will improve during the course of the test.

Major development efforts were mainly focused on subsystem A as it involves the integration of many important subsystems. The testing for the subsystem A was planned over three phases. The first phase is considered as a pre-development testing to estimate the initial reliability of the prototype in order to gauge the amount of development efforts required to meet the target reliability goals. The additional two phases focuses on meeting the final reliability target. Reliability testing for the subsystem B was also planned over three phases.

C. RELIABILITY GROWTH PLANNING METHODOLOGY

The first step in the reliability growth process is reliability growth planning. Reliability growth planning involves the development of an idealized growth curve. The major role of the idealized reliability growth curve is to quantify the overall development efforts so that the growth pattern can be evaluated relative to the basic objectives and resources. It also provides the program manager with a useful tool to monitor the reliability growth of the weapon system during its development.

The reliability of a system under development is generally increasing rapidly at the beginning and slows down towards the end. The idealized growth curve shown in Figure 5 depicts reliability growth as a smooth non-decreasing concave down curve with respect to time. A typical reliability test program consists of several test phases. Fitting a smooth curve to the proposed reliability values of the system at the end of each test phase, the resulting curve represents the overall pattern for reliability growth.

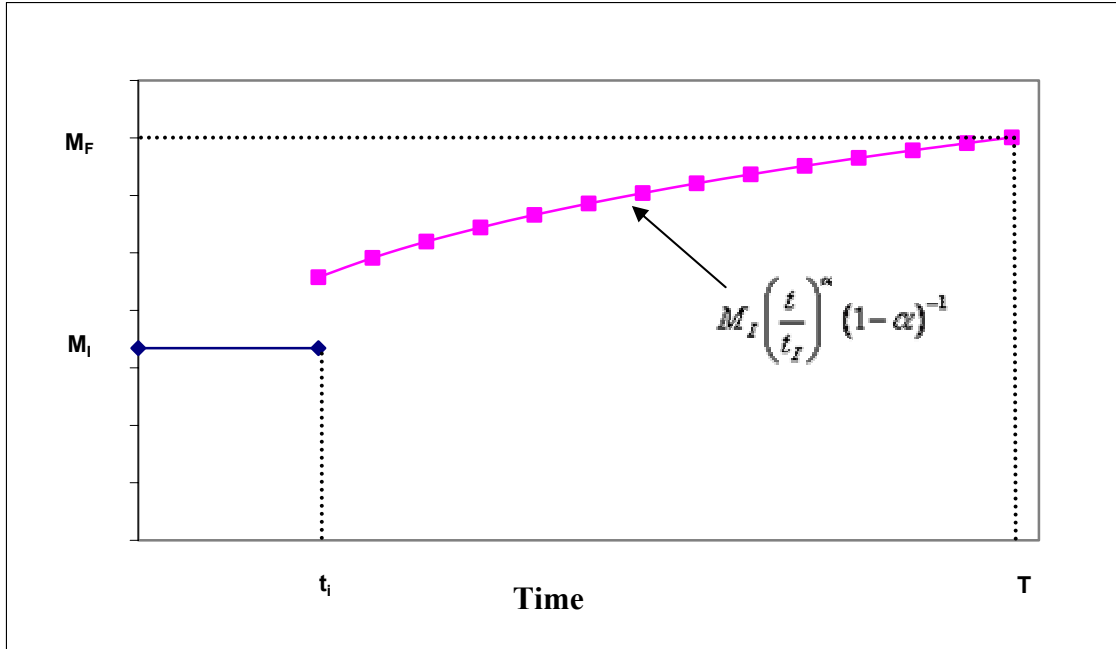


Figure 5. Example of an idealized growth curve

The formula for developing the idealized growth curve is based on Duane's model [Ref. 5].

$$M(t) = \begin{cases} M_I & 0 < t < T_i \\ M_I \left(\frac{t}{t_i} \right)^\alpha (1-\alpha)^{-1} & t > T_i \end{cases} \quad (3.1)$$

Where

M_F = Desired MTBF value at T

t = Cumulative test time

t_i = Cumulative test time at starting point

M_I = Average initial MTBF of the system at the beginning

α = System reliability growth rate between 0 and 1.0

The development of the idealized growth curve starts with the determination of the length of the initial test phase (t_i) and the average MTBF (M_i) over this initial test phase. The success in the development of the idealized growth curve depends on the ability to accurately estimate these parameters as they will affect the total test time and growth rate required to achieve the required reliability. A system with a lower initial average MTBF will require longer test time given a fixed growth rate.

There is no standard way of determining the values of these parameters. The average initial MTBF of the system, M_i , is the average MTBF over the initial test phase before any modification is developed, implemented or tested. The practice of arbitrarily choosing a starting point, such as 10% of the requirement is not recommended [Ref. 5]. One way of accurately determining these parameters is to perform an initial test so that M_i and T_i are known. The initial test phase of the RGT program is conducted to “stabilize” the test data, so it must be long enough for the first failure mode to surface.

The value M_F represents the desired MTBF at the end of the reliability growth test. The total amount of testing, T , is determined through a joint effort between the contractor and the program manager and it is derived based on considerations on available resources, and calendar time, as well as the number of prototypes available.

The growth rate of the system (α) determines the length of time needed to grow from the initial MTBF to the required MTBF. The growth rate gives an indication on how fast the system reliability is improving. The growth rate is governed by the efficiency by which failures are corrected. A large growth rate ($\alpha > 0.5$) reflects an aggressive reliability program while a low value of growth rate ($\alpha < 0.1$) reflects a program where no quick fixes are available.

For fixed values of T , M_F , M_i and t_i , the value of α may be approximated by solving the following equation:

$$\alpha = -\ln\left(\frac{t}{t_i}\right) - 1 + \left[\left(1 + \ln\left(\frac{t}{t_i}\right)^2 \right) + 2\ln\left(\frac{M_F}{M_i}\right) \right]^{1/2} \quad (3.2)$$

This is a reasonably good approximation when α is less than 0.4 [Ref. 16]. The more precise way to solve for the value of α in equation 3.1 is by using numerical methods, e.g. with MsExcel.

1. Development of the Idealized Growth Curve for Subsystem A

The development of the idealized growth curve is based on the initial estimate of the MTBF and the limitations constrained on testing such as number of units under test, resources and time available for testing. For subsystem A, the parameters for constructing the idealized growth curve are based on the given mission conditions.

A mission reliability of 200 rounds Mean-Rounds-Between-Failure (MRBF) was required at the end of the reliability growth test. Since this is a combat system, the total test time for this subsystem is expressed in terms of number of rounds instead of calendar time and it was limited to a maximum of 2300 rounds due to resource constraints available in the development program.

Average initial MRBF, (M_i). The initial MRBF is determined based on pre-developmental testing of the proposed system. The pre-development testing resulted in 4 mission affecting failures in 280 rounds. The MRBF was projected to be constant during this initial testing because no significant design changes were incorporated during the test, so the MRBF was estimated as:

$$\text{Initial MRBF} = \frac{280}{4} = 70 \text{ rounds} \quad (3.3)$$

Growth rate, (α). The initial MRBF is estimated to be 70 rounds and a final MRBF of 200 rounds is desired after 2300 rounds of testing. For this program, the first test phase is 280 rounds. The desired growth rate parameter can be determined from the following equation.

$$\alpha = -\ln\left(\frac{2300}{280}\right) - 1 + \left[\left(1 + \ln\left(\frac{2300}{280}\right) \right)^2 + 2 \ln\left(\frac{200}{70}\right) \right]^{1/2} \quad (3.4)$$

The growth rate, α , is found to be 0.32 for the given conditions, anything less would violate the resource constraints. The approximation of the α value of 0.32 in equation 3.4 is consistent with the results of the numerical method. An α value of 0.32 indicates a relatively aggressive development program that would require emphasis on the analysis and fixing of problem failure modes [Ref. 16]. Since major development efforts will be focused on the subsystem A, an α value of 0.32 is reasonable. The total test time is sensitive to the parameter α . As shown in table 4, using a test time of less than 2300 rounds would result in a projected α greater than 0.32 which means that it will require an even more aggressive reliability growth program.

M_i	70					
T_i	280					
α	0.3	0.32	0.34	0.36	0.38	0.4
T (rounds)	2880	2280	1780	1500	1280	1080

Table 4. Sensitivity analysis of α on total test duration

The test parameters of the reliability growth plan are summarized in Table 5 below.

	Subsystem A
Reliability Target (MRBF)	200 rounds
Total Test Duration	2300 rounds
Growth Rate	0.32

Table 5. Summary of test parameters for subsystem A

The plan assumed that the MRBF of subsystem A would grow from its initial level to the required 200 rounds MRBF in accordance to the following form of Duane's expression for reliability growth:

$$M(t) \left\{ \begin{array}{ll} 70 & 0 < t < 280 \\ 70 \left(\frac{t}{280} \right)^{0.32} (1-0.32)^{-1} & t > 280 \end{array} \right\} \quad (3.5)$$

T	M(t)
0	70
280 (-)	70
280 (+)	103
380	114
500	124
650	135
800	144
950	152
1100	159
1250	166
1400	172
1550	178
1700	183
1850	188
2000	193
2300	202

Table 6. Computed MRBF values for the idealized growth curve

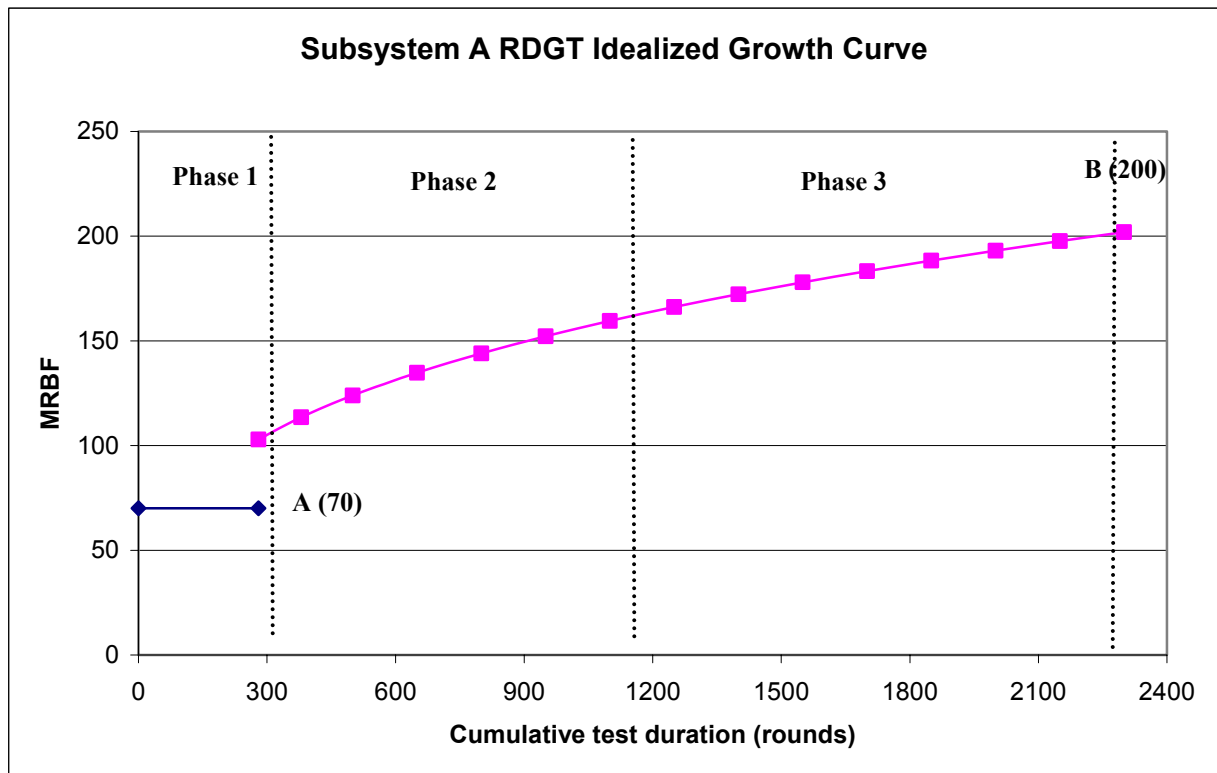


Figure 6. Idealized growth curve for subsystem A

The idealized growth curve for subsystem A is shown in Figure 6. The reliability growth test of subsystem A consists of two additional test phases at 280-1180 rounds and 1100-2300 rounds. More test time is being allocated to the last test phase as more time will be required to verify the effectiveness of the previous fixes.

2. Development of the Idealized Growth Curve for Subsystem B

The approach taken for developing the idealized growth curve for subsystem B is similar to that for the subsystem A. A mission reliability of 350 kilometers Mean-Kilometers-Between-Failure (MKBF) was required at the end of the reliability growth test. The total test time for the subsystem is expressed in terms of kilometers.

Average initial MKBF, (M_i): The initial MKBF was estimated during the prototype run-in test. The run-in test resulted in 6 mission affecting failures in 1000 kilometers. The MKBF was projected to be constant during this initial testing because no significant design changes were incorporated during the test, so the MKBF was estimated as:

$$\text{Initial MKBF} = \frac{1000}{6} = 167 \text{ kilometers} \quad (3.6)$$

Growth rate, (α) and total test time. The initial MKBF is estimated to be 167 kilometers and a final MKBF of 350 kilometers is desired at the end of the testing. Table 7 shows the various growth rates and the corresponding total test time computed based on the initial MKBF and test time.

M_i	167									
T_i	1000									
α	0.25	0.26	0.27	0.28	0.29	0.3	0.32	0.34	0.36	0.38
T (km)	6150	5450	4850	4350	3950	3600	3050	2600	2270	2000

Table 7. Growth rate versus total test duration

Based on schedule constraints, the maximum allowable test time was approximately 4850 kilometers. The corresponding desired growth rate is 0.27. The approximation of the α value of 0.27 in equation 3.4 is consistent with the results of the numerical method.

	Subsystem B
Reliability Target (MKBF)	350 kilometers
Total Test Duration	4850 kilometers
Growth Rate	0.27

Table 8. Summary of test parameters for subsystem B

The plan assumed that the MKBF would grow from its initial level to the required 350 kilometers MKBF in accordance to the following form of Duane's expression for

$$\text{reliability growth } M(t) \begin{cases} 167 & 0 < t < 1000 \\ 167 \left(\frac{t}{1000} \right)^{0.27} (1 - 0.27)^{-1} & t > 1000 \end{cases} \quad (3.7)$$

T	M(t)
0	167
1000 (-)	167
1000 (+)	229
1300	246
1600	260
1900	272
2200	283
2500	293
2800	302
3100	310
3400	318
3700	326
4000	333
4300	339
4600	345
4850	350

Table 9. Computed MKBF values for the idealized growth curve

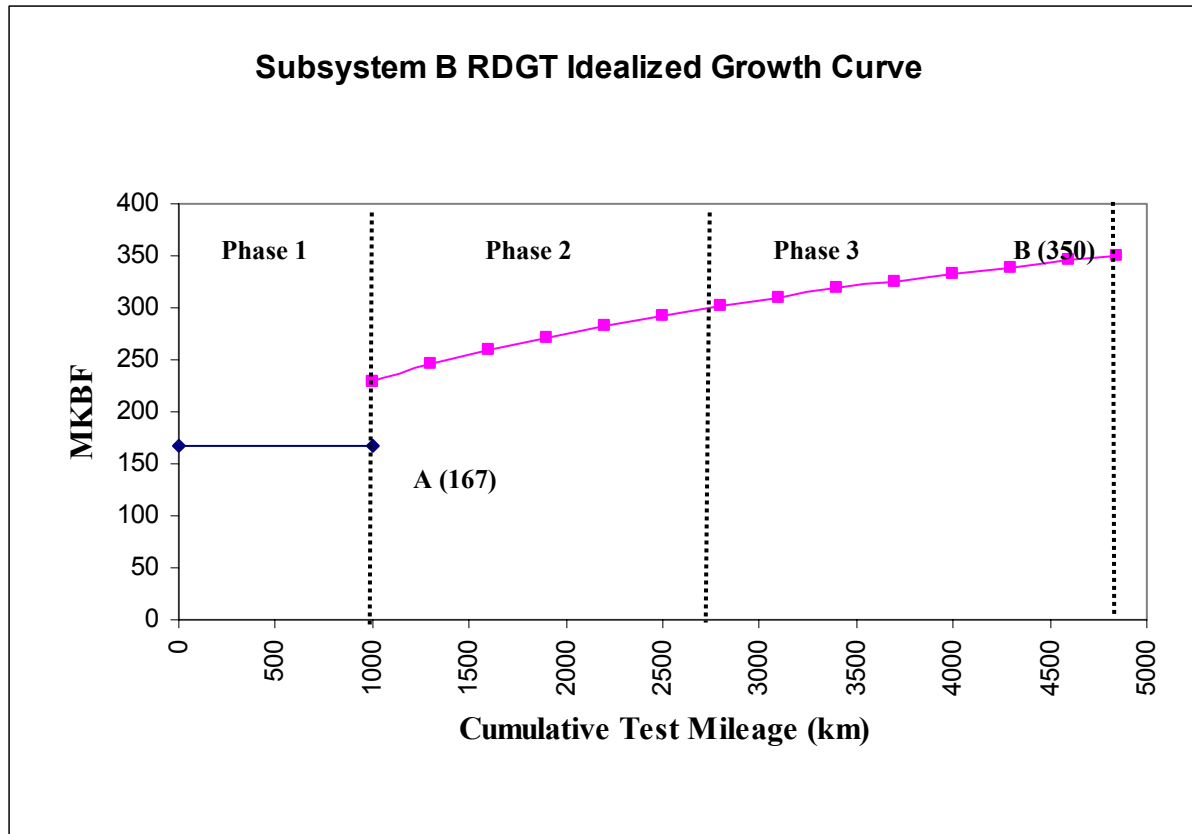


Figure 7. Idealized growth curve for the subsystem B

The idealized growth curve for subsystem B is shown in Figure 7. Similarly, the reliability growth test of the chassis consists of two additional test phases at 1000-2600 kilometers and 2600-4850 kilometers. More test time is being allocated to the last test phase as more time will be required to verify the effectiveness of the previous fixes. As compared to subsystem A, a lower α value of 0.27 for subsystem B is reasonable since it is an Off-The-Shelf (OTS) system.

THIS PAGE INTENTIONALLY LEFT BLANK

IV. RESULTS AND DISCUSSION OF RELIABILITY GROWTH ANALYSIS

A. INTRODUCTION

This chapter first introduces the reliability growth models used for the reliability growth analysis of the combat system and follows with the results and discussion. The objectives of the reliability growth analysis include:

1. Estimating the demonstrated MRBF and MKBF of the two subsystems at the end of each test phase.
2. Projecting the MRBF and MKBF of the subsystems if delayed fixes were incorporated at the end of a test phase.
3. Generate reliability growth plots (e.g. MTBF vs Time) to determine if reliability is improving, decreasing or constant.

The demonstrated MRBF or MKBF provide an estimate for the system configuration on test at the end of a test phase. This value is determined by analysis of the test results using AMSAA reliability growth models. The demonstrated value is then compared to the idealized growth curve at the end of each test phase to determine if reliability growth is progressing satisfactorily.

A projected reliability value is an estimation of the increased in system reliability by taking into account the effect of delay fixes.

Equations 4.1 to 4.24 in the following sections are taken from Reference 20, and were formulated by Dr. Larry Crow.

B. AMSAA RELIABILITY GROWTH MODELS

There are three types of AMSAA growth models used for reliability growth analysis. They are 1) AMSAA Basic Model for Test-Fix-Test 2) AMSAA Projection

Model for Test-Find-Test and 3) AMSAA Extended Model for Test-Fix-Find-Test [Ref. 20]. The distinction between these three models is when fixes are incorporated into the system.

The test-fix-test model is employed when a corrective action is immediately found for a failure mode and is incorporated into the system, which is then retested to verify its effectiveness and to surface new failure modes. This model estimates the achieved reliability of the system after all fixes have been incorporated into the system before the end of a test phase. However, it cannot estimate the increased in reliability due to delayed fixes that were incorporated at the end of a test.

The test-find-test model is employed when corrective actions for all surfaced failure modes are incorporated into the system at the end of the test. These corrective actions results in a distinct jump in system reliability. This model estimates the jump in reliability due to delayed fixes.

The test-fix-find-test model is a combination of the two types discussed above. It is employed when some corrective actions are incorporated into the system during the test while some are delayed until the end of the test.

It is important to note that the choice of model for analysis should not be determined by the data but rather a realistic assessment of the test program's corrective actions.

1. AMSAA Basic Model for Test-Fix-Test

The AMSAA model employs the Weibull process to model reliability growth during a developmental phase. This model was formulated by Dr. Larry Crow and it is frequently used on systems when usage is measured on a continuous scale. It is also designed for tracking reliability within a test phase and not across test phases [Ref. 19]. The test-fix-test model evaluates reliability growth that results from the introduction of design fixes into the system during a particular test phase.

The AMSAA test-fix-test model assumes that system failures during a development testing phase follow the non-homogeneous Poisson Process (NHPP) with a Weibull intensity function of the following form:

$$r(t) = \lambda \beta t^{\beta-1} \quad (4.1)$$

t = cumulative test time

λ = the scale parameter. It depends on the unit of measurement chosen for t

β = the shape parameter (also known as the growth parameter) because it characterizes the shape of the graph of the intensity function

The relationship between the growth rate and shape parameter is given as:

$$\alpha_{DUANE} = 1 - \beta_{AMSAA} \quad (4.2)$$

Suppose development testing for a particular test phase stops at time T and no further improvements are being made into the system. In other words, the system configuration is fixed after time T . The demonstrated or achieved failure intensity is

$$\hat{\lambda}_{CA} = r(T) = \hat{\lambda} \hat{\beta} T^{\hat{\beta}-1}. \quad (4.3)$$

The demonstrated instantaneous MTBF at the end of the test phase after T units of testing is given as the reciprocal of the intensity function:

$$\hat{M}_{CA} = \frac{1}{\hat{\lambda} \hat{\beta} T^{\hat{\beta}-1}} \quad (4.4)$$

β is a very important parameter as it indicates whether there is reliability growth during the development process. Three possible conditions are reflected by the value of β

$\beta < 1$: Positive reliability growth because failure rate is decreasing

$\beta = 1$: The constant case. No reliability growth because failure rate is constant

$\beta > 1$: Negative reliability growth because failure rate is increasing with time

If the testing were stopped at time T and significant modifications are made on the system, there may be a jump in system's reliability. However, the AMSAA test-fix-test model does not estimate the jump due to these delayed fixes.

Parameters Estimation using method of Maximum Likelihood

Estimates of the two parameters β and λ are made using on the method of maximum likelihood in the MIL-HDBK-189 [Ref.5]. They are estimated based on times to failure data which has been accumulated during a given test phase. It is important then to collect the actual times to failure and total test time during development testing. The estimate of the shape parameter β , is given by

$$\hat{\beta} = \frac{N}{N \ln T - \sum_{i=1}^N \ln X_i} \quad (4.5)$$

N = Total number of failure occurrences

T = Total accumulated test time

X_i = Cumulative test time at which the i th failure occurred

The scale parameter is given by

$$\hat{\lambda} = \frac{N}{T^{\hat{\beta}}} \quad (4.6)$$

Cramer-Von Mises Goodness of Fit Test

Next, the Cramer-Von Mises goodness of fit test is performed to determine if there is enough information to reject the hypothesis that the reliability growth process can be described by the AMSAA model [Ref.5]. The Cramer-Von Mises statistics is given by the following expression:

$$C_M^2 = \frac{1}{12M} \sum_{i=1}^M \left[\left(\frac{X_i}{T} \right)^{\hat{\beta}} - \frac{2i-1}{2M} \right]^2 \quad (4.7)$$

M = number of failures

If the statistics C_M^2 exceeds the critical value corresponding to M for a chosen significant level, then the null hypothesis that the AMSAA model adequately described the growth process shall be rejected. Otherwise, the model shall be accepted.

2. AMSAA Projection Model for Test-Find-Test

The AMSAA Projection Model for Test-Find-Test classifies all failure modes into two groups [Ref.20]:

Type A failure modes. No corrective actions will be taken for Type A failure modes. Type A failure mode has a constant failure intensity, λ_A .

Type B failure modes. Failure modes whose corrective actions will only be taken at the end of the test.

For the test-find-test model, the system failure intensity is constant ($\beta = 1$) during the test because no corrective actions are incorporated into the system. The system then experiences a jump in reliability after the incorporation of delayed fixes. The achieved system failure rate λ_s , prior to the delay fixes can be estimated as follows:

$$\hat{\lambda}_s = \hat{\lambda}_A + \hat{\lambda}_B \quad (4.8)$$

$$\hat{\lambda}_A = \frac{\text{Total number of Type A failures}}{\text{Total test time}} = \frac{N_A}{T} \quad (4.9)$$

$$\hat{\lambda}_B = \frac{\text{Total number of Type B failures}}{\text{Total test time}} = \frac{N_B}{T} \quad (4.10)$$

The projected failure intensity after the incorporation of delayed fixes is obtained by assigning an effectiveness factor (EF) d_j to every individual unique Type B failure modes. The assigned effectiveness factor based on engineering assessment results in a fractional decrease in the failure rate λ_j of the j-th Type B failure mode after fixes have been incorporated. The total number of Type B failures observed during a test is

$$N_B = \sum_{j=1}^M N_j \quad (4.11)$$

M = Total number of unique Type B failure modes and

N_j = Total number of failures for the j-th observed distinct Type B mode.

The projected failure intensity is then computed as follows:

$$\hat{\lambda}_p = \hat{\lambda}_A + \sum_{j=1}^M (1 - d_j) \frac{N_j}{T} + \bar{d}\hat{h}(T) \quad (4.12)$$

$$\bar{d} = \text{Average EF} = \frac{\sum_{j=1}^M d_j}{M} \quad (4.13)$$

$$h(T) = \hat{\lambda}\hat{\beta}T^{\beta-1} \quad (4.14)$$

$\hat{\lambda}$ and $\hat{\beta}$ are calculated using equation 4.5 and 4.6 based only on the M first occurrence failure times of the seen and unique Type B failure modes [Ref. 20].

The objective of this model is to estimate the jump in MTBF which is the inverse of the projected failure intensity given by

$$\hat{M}_p = \left[\hat{\lambda}_p \right]^{-1} \quad (4.15)$$

3. Extended Reliability Growth Model for Test-Fix-Find-Test

The Extended Model utilizes A, BC and BD failure mode classification to analyze reliability growth projection data [Ref. 20].

Type BD failure modes. Corrective actions for Type BD failure modes are delayed till the end of the test. They are the same as Type B failure modes in the test-find-test model.

Type BC failure modes. Corrective actions for Type BC failure modes are incorporated during the test.

Type A failure modes, as before, are those that will not receive any correction actions. Type A and Type BD failure modes do not contribute to reliability growth during the test. The growth in reliability during the test is affected only by corrective actions for Type BC failure modes. The objective of this model is to estimate the increased in reliability due to the corrective actions for Type BD failure modes at the end of the test.

The projected failure intensity after the incorporation of delayed fixes into the system for the Extended Model is

$$\hat{\lambda}_{EM} = \hat{\lambda}_{CA} - \hat{\lambda}_{BD} + \sum_{j=1}^M (1 - d_j) \frac{N_j}{T} + \bar{d} \hat{h}(T / BD) \quad (4.16)$$

The first term $\hat{\lambda}_{CA}$ is the failure rate prior to delay fixes. It is the same as equation 4.3 applied to all A, BC and BD failure modes. The remaining terms are calculated in the same manner as the AMSAA Test-Find-Test model using only data for BD failure modes.

Finally the projected MTBF after the incorporation of delayed fixes into the system for the Extended Model is the inverse of the failure intensity given by

$$\hat{M}_{EM} = \left[\hat{\lambda}_{EM} \right]^{-1} \quad (4.17)$$

In addition, the AMSAA Extended Test-Fix-Find-Test Model can be modified to analyze test-fix-test data and test-find-test data by designating failure modes as BC and BD respectively.

C. RELIABILITY GROWTH ANALYSIS FOR SUBSYSTEM A

Reliability growth for subsystem A is tracked over three phases of testing. Reliability is tracked on a phase by phase basis using test data collected within each test phase. The ReliaSoft's RGA 6 PRO software is used for analyzing the collected data and generating reliability growth plots [Ref. 21]. The type of reliability growth model selected for must be based on the type of management approach employed in each test phase:

Phase 1: AMSAA Extended Test-Find-Test Projection Model

Phase 2: AMSAA Extended Model for Test-Fix-Test

Phase 3: AMSAA Extended Model for Test-Fix-Find-Test

The AMSAA Basic Model for Test-Fix-Test does not utilize any failure mode designation but the AMSAA Extended Model does. Specific knowledge on Type BC and Type BD failure mode can help to generate useful metrics for decision making and engineering purposes [Ref. 20]. The AMSAA Extended Models are used to analyze both test-find test and test-fix-test data by setting all failure modes to BC and BD respectively. The underlying mathematical principles of the AMSAA Basic Test-Fix-Test Model and AMSAA Basic Test-Find-Test Model remain unchanged.

1. Phase 1 results and analysis

In Phase 1, the prototype system was subjected to 280 rounds of testing according to the test plan. Since this test phase is short, fixes are not incorporated into the system during the test. During the test, three failures were identified but all corrective actions were delayed till the end of the test. This management strategy is known as test-find-test. The AMSAA Extended Test-Find-Test Projection Model is selected to analyze the reliability of the system after the incorporation of delayed fixes. All failure modes identified during the test will receive a delay corrective action therefore all failures are

being classified as Type BD. These failures were also assigned a failure category according to their root cause as shown in Table 10.

j	Time to Event, X_j	Classification	Mode	Failure Category
1	21	BD	1	Faulty component
2	132	BD	2	Design
3	215	BD	3	Design

Table 10. Test-find-test data for Phase 1

BD Mode	Number of Failures, N_j	Time to First Occurrence	EF, d_j
1	1	21	0.65
2	1	132	0.7
3	1	215	0.7

Table 11. Test-find-test Type B failure mode data and EF for Phase 1

Table 11 shows the frequency and the assigned effectiveness factor (EF) for each Type BD failure mode. The EF is an engineering estimate based on the probability that the fix is effective in mitigating or reducing the probability of occurrence for the particular failure mode. An EF of 1.0 is not practical in most cases since a fix will unlikely be able to completely eliminate a failure mode. Studies have shown that an average effectiveness factor of 0.7 is reasonable for a typical reliability growth program. [Ref. 20] Failure Mode Type BD1 was assigned a lower EF due to high uncertainty associated with the effectiveness of the correction action.

Since the test data consists of only Type BD failure modes, the achieved system failure intensity can be estimated by equation 4.8.

$$\hat{\lambda}_s = \hat{\lambda}_{BD} = \frac{N_B}{T} = \frac{3}{280} = 0.0107$$

The estimated achieved MRBF at T=280 rounds before the jump is the inverse of the achieved system failure intensity.

$$\hat{M}_s = \frac{1}{\hat{\lambda}_s} = 93.3 \text{ rounds}$$

Next, the projected failure intensity due to the delay fixes is calculated using equation 4.12.

$$\hat{\lambda}_p = \hat{\lambda}_A + \sum_{j=1}^M (1 - d_j) \frac{N_j}{T} + \bar{d} \hat{h}(T)$$

The average EF of the delay fixes is given in equation 4.13

$$\bar{d} = \text{Average EF} = \frac{\sum_{j=1}^M d_j}{M} = \frac{0.65 + 0.7 + 0.7}{3} = 0.683$$

The term $\hat{h}(T / BD) = \hat{\lambda} \hat{\beta} T^{\beta-1}$ from equation 4.14 is a function of $\hat{\beta}$ and $\hat{\lambda}$. These two parameters are estimated from equations 4.5 and 4.6 using first occurrence data from Table 11.

$$\hat{\beta} = \frac{N}{N \ln T - \sum_{i=1}^N \ln X_i} = \frac{3}{[3 \ln 280 - (\ln 21 + \ln 132 + \ln 215)]} = 0.8319$$

$$\hat{\lambda} = \frac{N}{T^{\hat{\beta}}} = \frac{3}{280^{0.831}} = 0.0276$$

$$\hat{h}(280 / BD) = 0.0089$$

This metric $\hat{h}(T / BD)$ represents the intensity for Type BD failure modes that have not been seen during the testing which also means the rate at which new distinct Type BD modes are occurring at the end of the test.

With all the above parameters defined, the projected failure intensity can be calculated.

$$\hat{\lambda}_p = \hat{\lambda}_A + \sum_{j=1}^M (1 - d_j) \frac{N_j}{T} + \bar{d} \hat{h}(T) = \sum_{j=1}^3 (1 - d_j) \frac{N_j}{280} + 0.683 * 0.0089 = 0.00952$$

The projected MRBF due to the jump is the inverse of the project

$$\hat{M}_p = \frac{1}{\hat{\lambda}_p} = 105 \text{ rounds}$$

For a two-sided confidence level of 90 %, the projected MRBF is between 40 and 278 rounds.

Projection Summary				
β :	0.8319		PMTBF:	105.4
$\hat{\lambda}$:	0.0276		DMTBF:	93.33
Statistical Results				
	Result		Test Value	Upper
Cram'er Von Mises (BD)	Passed		0.059	0.154

Table 12. RGA 6 PRO projection summary and Cramer Von Mises test results for Phase 1

The RGA 6 PRO generated results as shown in Table 12 is similar to the hand calculated values. The Cramer-Von Mises statistics of 0.059 is below the critical value of 0.154 for a significance level of 0.1. Hence the hypothesis that the AMSAA model is applicable is accepted.

Figure 8 shows the plot of reliability versus time for subsystem A during the test. The MRBF is constant ($\beta = 1$) during the test because no fixes were implemented on the system and thus the system failure rate remains constant during the test. There is a jump in reliability at the end of the test due to fixes being incorporated into the system. The projection model estimates that the system MRBF jumps to a value of 105 rounds due to three distinct corrective actions with the corresponding EF stated in Table 11. The estimated MRBF of 106 rounds after the incorporation of fixes has exceeded the planned target of 104 rounds at the end of Phase 1.

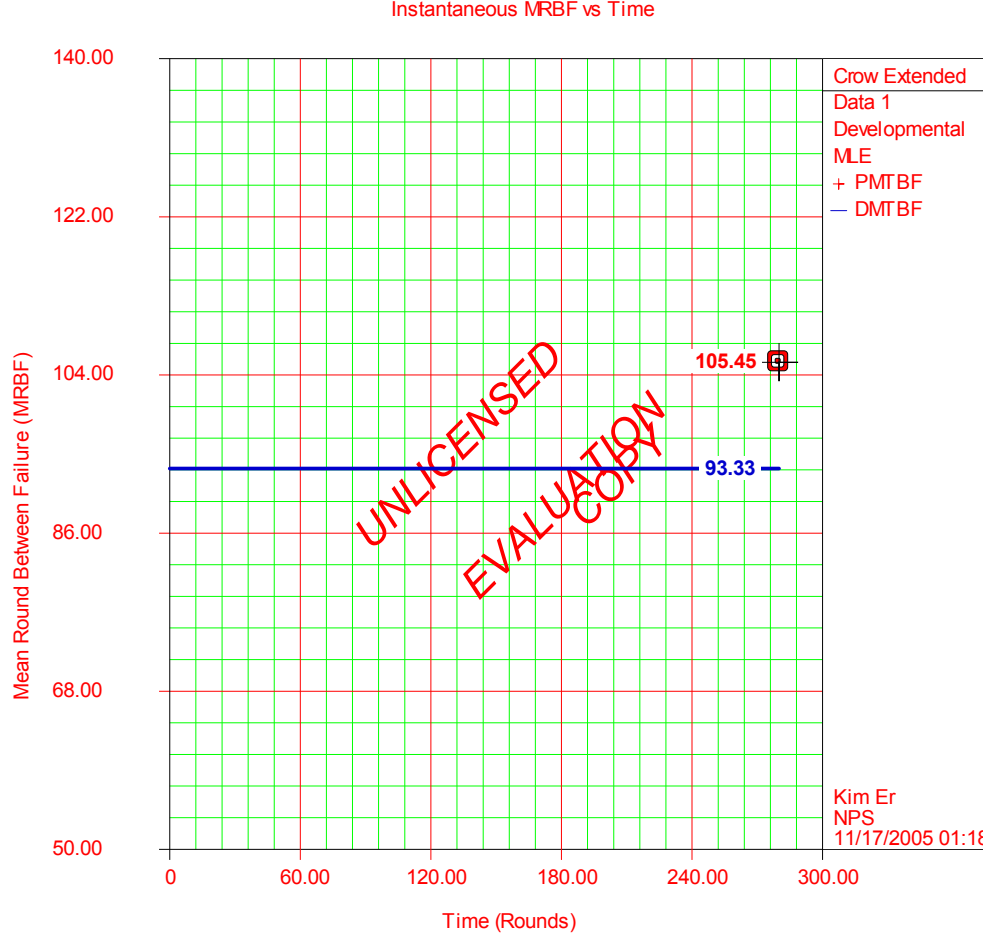


Figure 8. MRBF projection for Phase 1

In addition, the AMSAA Extended Test-Find-Test Projection Model can also be used to estimate the fraction of seen and unseen Type BD failure intensity at the end of the test. The intensity for Type BD failure modes that have been seen in the testing can be estimated as follows:

$$\hat{\lambda}_{BD} - \hat{h}(280 / BD) = 0.0107 - 0.0089 = 0.0018 \quad (4.18)$$

The fraction of Type BD failure intensity due to failure modes that have been seen in test is [Ref. 20]:

$$\text{Fraction Seen} = \frac{0.0018}{\hat{\lambda}_{BD}} = 0.168 \quad (4.19)$$

The fraction of Type BD failure intensity due to failure modes that have not been seen in test is [Ref. 20]:

$$\text{Fraction Unseen} = 1 - \frac{\hat{h}(280 / BD)}{\hat{\lambda}_{BD}} = 0.831 \quad (4.20)$$

Figure 9 displays the failure rate for each Type BD failure modes before and after implementing the fixes. It provides a clear visibility on the failure rate breakdown of each individual Type BD failure mode to the system's overall failure rate. Failure mode BD1 appears to have the highest failure rate from Figure 9 as it is directly dependent on the assumed EF. In this case, the EF for failure mode BD1 has been assumed a lower value as compared to BD2 and BD3 and should be the main focus in the failure management strategy. The ability to designate failure modes has certainly provided clearer management and engineering insights when formulating the failure management strategy.

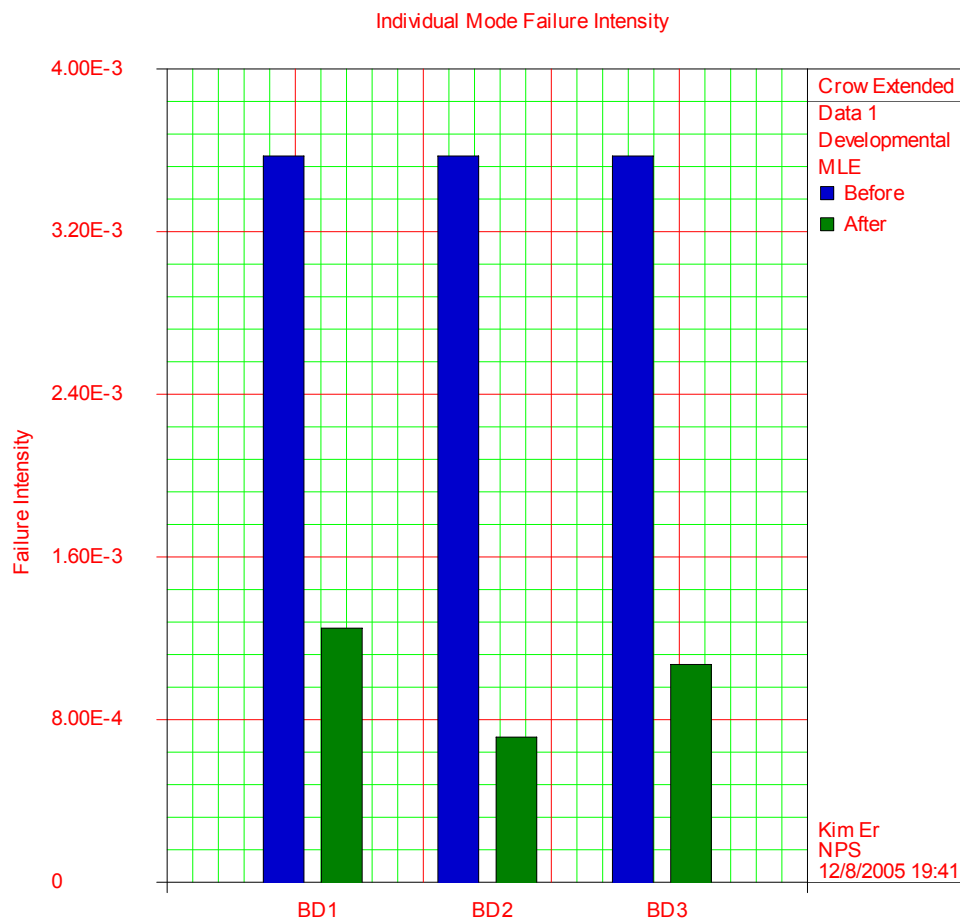


Figure 9. Before and after failure rate for Type BD failure modes in Phase 1 based on frequency and EF

2. Phase 2 results and analysis

The testing approach used in Phase 2 is Test-Analyze-And-Fix (TAAF), in which fixes for all failure modes discovered are being incorporated during the test. The system is tested for 820 rounds in this phase. The AMSAA Extended Test-Fix-Test Model designates all failures as Type BC as shown in Table 13.

j	Time to Event, X_j	Classification	Mode	Failure Category
1	27	BC	1	Faulty component
2	72	BC	2	Design
3	122	BC	2	Design
4	265	BC	3	Software
5	317	BC	4	Design
6	394	BC	5	Design
7	455	BC	2	Design
8	719	BC	6	Faulty component

Table 13. Test-fix-test data for Phase 2

BC Mode	Number of Failures, N_j	Time to First Occurrence
1	1	27
2	3	72
3	2	275
4	1	317
5	1	394
6	1	719

Table 14. Unique first time occurrence BC failure mode for Phase 2

During Phase 2, six unique Type BC failure modes were observed in eight hundred and twenty rounds of testing. The demonstrated MRBF calculations will be calculated next.

The shape parameter is estimated using equation 4.5

$$\hat{\beta} = \frac{N}{N \ln T - \sum_{i=1}^N \ln X_i}$$

$$= \frac{8}{\left[8 \ln 820 - (\ln 27 + \ln 72 + \ln 122 + \ln 265 + \ln 317 + \ln 394 + \ln 455 + \ln 719) \right]}$$

$$= 0.7089$$

The calculated $\hat{\beta}$ of 0.7089 ($\hat{\beta} < 1$) implies positive and improved reliability growth in this phase.

The relationship between the growth rate and the shape parameter is given by equation 4.2.

$$\alpha_{DUANE} = 1 - \beta_{AMSA} = 1 - 0.7089 = 0.2911$$

The calculated growth rate of 0.2911 is close to but falls below the desired value of 0.32. It implies that reliability growth is not growing as fast as it was planned to be.

The scale parameter is estimated using equation 4.6.

$$\hat{\lambda} = \frac{N}{T^{\hat{\beta}}} = \frac{8}{820^{0.7089}} = 0.0687$$

The achieved failure intensity is given by equation 4.3.

$$\hat{\lambda}_{CA} = r(T) = \hat{\lambda} \hat{\beta} T^{\hat{\beta}-1} = 0.0687 * 0.7089 * 820^{0.7089-1} = 0.0069$$

The demonstrated instantaneous MRBF at the end of phase 2 after 820 rounds of testing is the reciprocal of the intensity function given by equation 4.4.

$$\hat{M}_{CA} = \frac{1}{\lambda_{CA}} = 145 \text{ rounds}$$

For a two-sided confidence level of 90 %, the demonstrated MRBF is between 63 and 431 rounds.

Another useful metric that can be determine from the test data is the initial system MRBF at the beginning of this phase [Ref.20].

$$M_I = \frac{\Gamma\left(1 + \frac{1}{\hat{\beta}}\right)}{\hat{\lambda}^{\frac{1}{\hat{\beta}}}} = 54 \text{ rounds} \quad (4.21)$$

The initial MRBF of 54 rounds at the beginning of Phase 2 falls within the confidence interval of 40 and 280 rounds at the end of Phase 1. At the beginning of the test it is estimated that the initial system MRBF was 54 rounds and due to six distinct fixes the reliability grew to 145 rounds at the end of 820 rounds of test.

Analysis Summary				
Model:	Crow-AMSAA (NHPP)		Analysis Method:	MLE
β :	0.7089		Test Procedure:	Developmental
λ :	0.0688		Input Type:	Cumulative
Growth Rate:	0.2911		Termination Time:	820
Instant. MTBF:	144.58			
Statistical Results				
	Result		Test Value	Upper
Cram'er Von Mises	Passed		0.035	0.165

Table 15. RGA 6 PRO analysis summary and Cramer Von Mises test results for Phase 2

The RGA 6 PRO generated results presented in Table 15 are consistent with the hand calculated values. The Cramer-Von Mises statistics of 0.035 is below the critical value of 0.165 for a significance level of 0.1. Hence the hypothesis that the AMSAA model is appropriate is accepted.

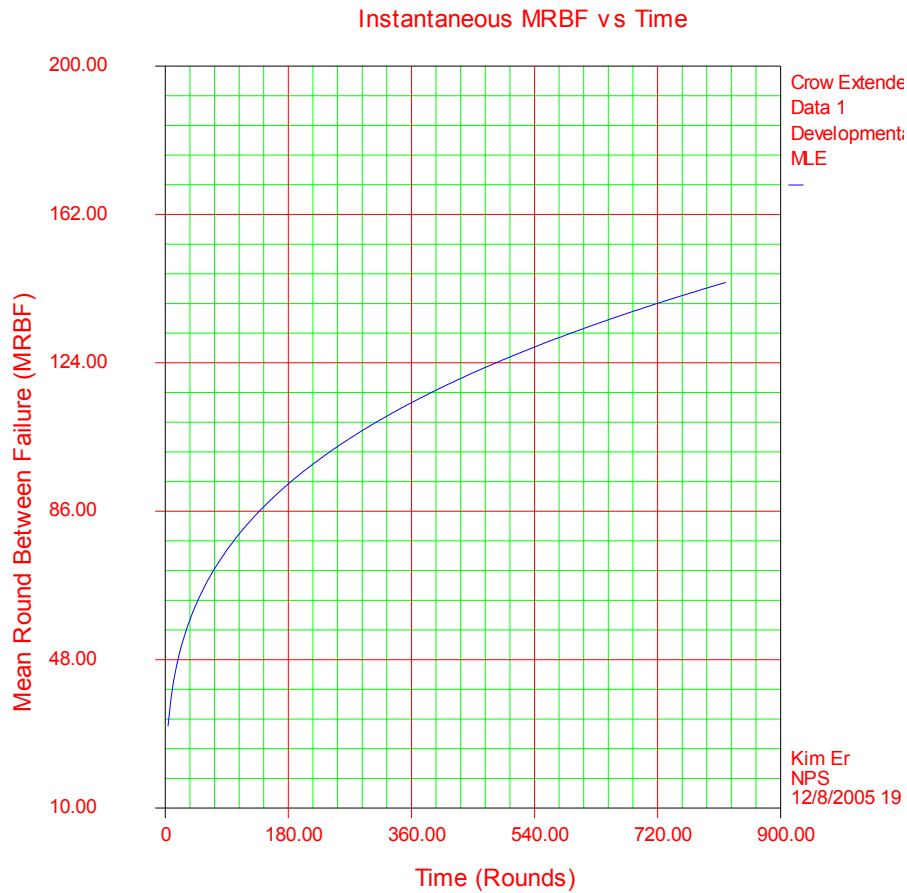


Figure 10. MRBF projection for Phase 2

Figure 10 indicates that reliability is increasing with time. The effective application of the TAAF approach in surfacing and fixing failure modes has contributed to reliability growth in this phase. According to the idealized growth curve, the expected MRBF at the end of Phase 2 should approach 159 rounds. The demonstrated MRBF of 145 rounds is close to approaching the expected target.

However one main concern identified in this phase is the relative high frequency of mode BC2 as shown in Figure 11. An effective failure management strategy at this point of the program should focused on fixing on failure mode BC2 by allocating more resources to identify its root cause and improve on current corrective actions.

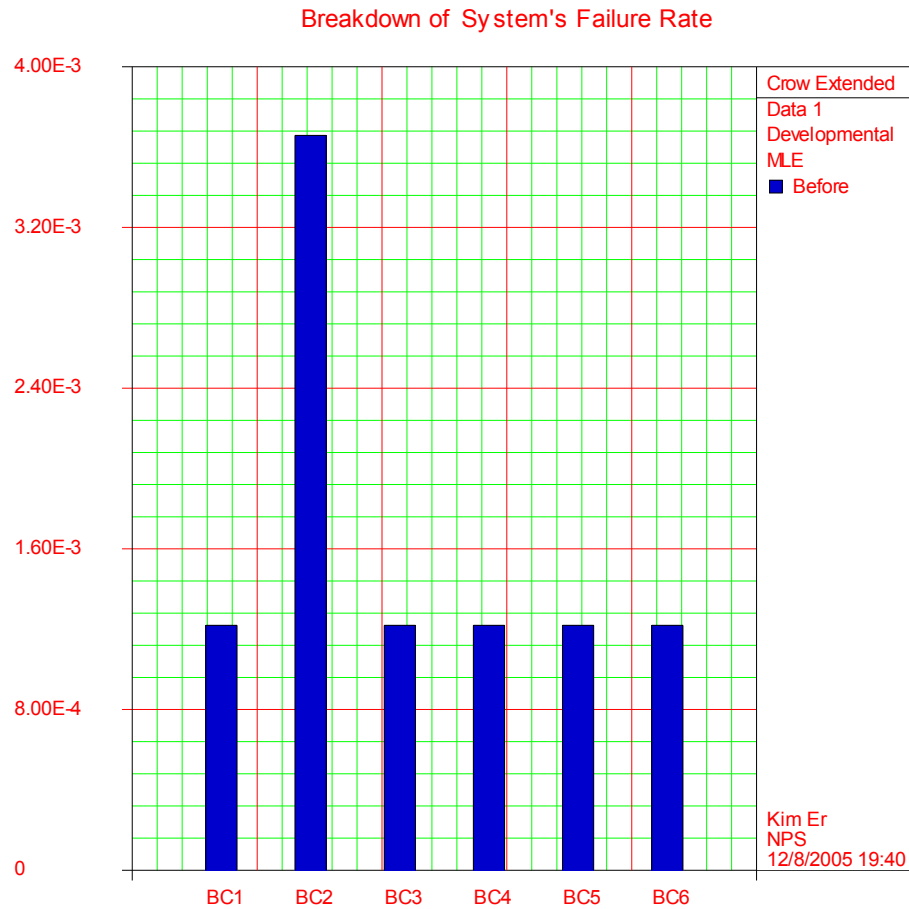


Figure 11. Failure rate for individual BC failure modes after the test

3. Phase 3 results and analysis

In Phase 3, some fixes are incorporated into the system during the test while others are delayed until the end of the test. The reasons for the delayed fixes are due to: 1) unavailability of spares parts or tools required for component replacement or repair and 2) inability to identify the root cause of failure during the test. This type of data is a combination of test-fix-test and test-find-test which is known as test-fix-find-test. The AMSAA Extended Test-Fix-Find-Test Model is used for analyzing the data. There are nine failures observed in 1200 rounds of testing. The failures that receive a correction action during the test are classified as BC while those that are delayed will be classified as BD. All the failures surfaced in this phase are presented in Table 16.

j	Time to Event, X_j	Classification	Mode	Failure Category
1	55	BD	1	Faulty component
2	101	BC	1	Design
3	212	BC	1	Software
4	317	BC	2	Faulty component
5	379	BC	3	Software
6	465	BC	4	Design
7	520	BD	2	Faulty component
8	579	BD	3	Quality
9	900	BC	5	Workmanship

Table 16. Test-fix-find-test data for Phase 3

BD Mode	Number of Failures, N_j	Time to First Occurrence	EF, d_j
1	1	55	0.6
2	1	520	0.6
3	1	579	0.6

Table 17. Test-find-test Type BD failure mode data and EF for Phase 3

There are six unique BC failure modes and three unique BD failure modes in this phase. The EF for all BD failure modes is conservatively assigned as 0.6 because this the last test phase with no further testing to verify their effectiveness. The assigned EF will be used for estimating the jump in the system reliability due to the delay fixes.

The estimate of the failure intensity after 1200 rounds of testing before incorporation of delayed fixes is estimated using equation 4.3.

$$\hat{\lambda}_{CA} = r(T) = \hat{\lambda}\hat{\beta}T^{\hat{\beta}-1}$$

The shape parameter $\hat{\beta}$ is calculated using equation 4.5 based on the data in Table 15

$$\hat{\beta} = \frac{N}{N \ln T - \sum_{i=1}^N \ln X_i}$$

=

$$\frac{9}{\left[9 \ln 1200 - (\ln 55 + \ln 101 + \ln 212 + \ln 317 + \ln 379 + \ln 465 + \ln 520 + \ln 579 + \ln 900) \right]}$$

$$= 0.715$$

The calculated $\hat{\beta}$ of 0.715 ($\hat{\beta} < 1$) implies positive reliability growth in this phase.

The growth rate is given by equation 4.3

$$\alpha_{DUANE} = 1 - \beta_{AMSA} = 1 - 0.715 = 0.285$$

The calculated growth rate of 0.285 is consistent with that of Phase 2.

The scale parameter is given by equation 4.6

$$\hat{\lambda} = \frac{N}{T^{\hat{\beta}}} = \frac{9}{1200^{0.715}} = 0.0563$$

The achieved failure intensity before the incorporation of the delay fixes at a cumulative time of 1200 rounds is

$$\hat{\lambda}_{CA} = r(T) = \hat{\lambda} \hat{\beta} T^{\hat{\beta}-1} = 0.0563 * 0.715 * 1200^{0.715-1} = 0.00533$$

The achieved MRBF is the inverse of the failure intensity given by

$$\hat{M}_{CA} = \left[\hat{\lambda}_{CA} \right]^{-1} = 186 \text{ rounds}$$

For a two-sided confidence level of 90 %, the demonstrated MRBF is between 85 and 512 rounds.

Analysis Results				
β :	0.715		DMTBF:	186.3
$\hat{\lambda}$:	0.0563			
Statistical Results				
	Result		Test Value	Upper
Cram'er Von Mises	Passed		0.0995	0.167

Table 18. RGA 6 PRO failure modes analysis results and Cramer Von Mises statistical test results for Phase 3

The RGA 6 PRO generated results presented in Table 18 are consistent with the hand calculated values. The Cramer-Von Mises statistics of 0.0727 is below the critical value of 0.16 for a significance level of 0.1. Hence the hypothesis that the AMSAA model is appropriate is accepted.

The demonstrated MRBF of 186 rounds at the end of Phase 3 prior to the incorporation of fixes did not meet the requirement of 200 rounds because the achieved growth rate of 0.29 is below the planned value of 0.32. However a trend of decreasing number failures is obvious from the cumulative number of failures versus time plot in Figure 12. There is only one failure observed in the last 600 rounds of testing. Figure 12 also shows that the results are slightly biased as the number of failures at each instant of time is being underestimated. The next step is to estimate the jump in reliability as a result of delayed fixes.

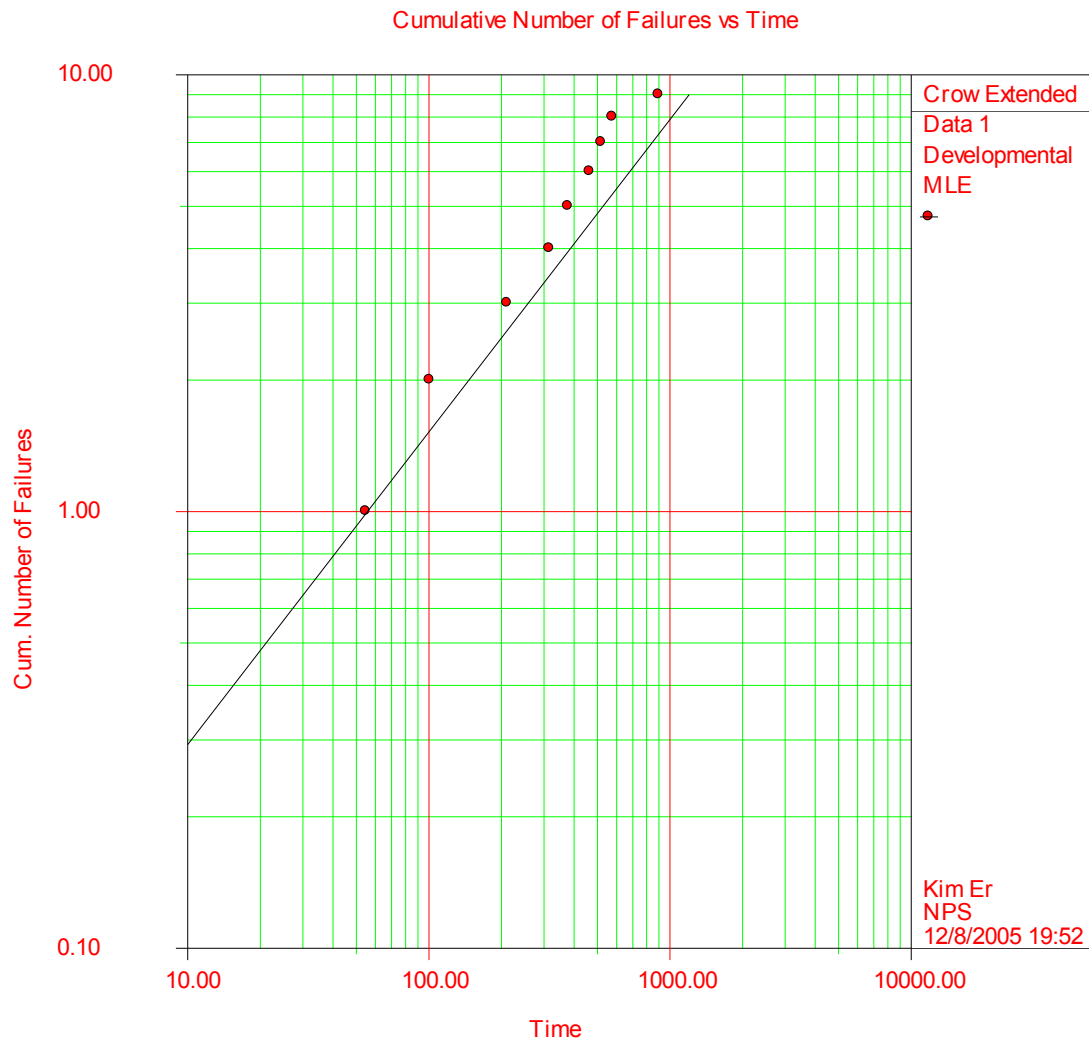


Figure 12. Cumulative number of failures vs time plot for Phase 3

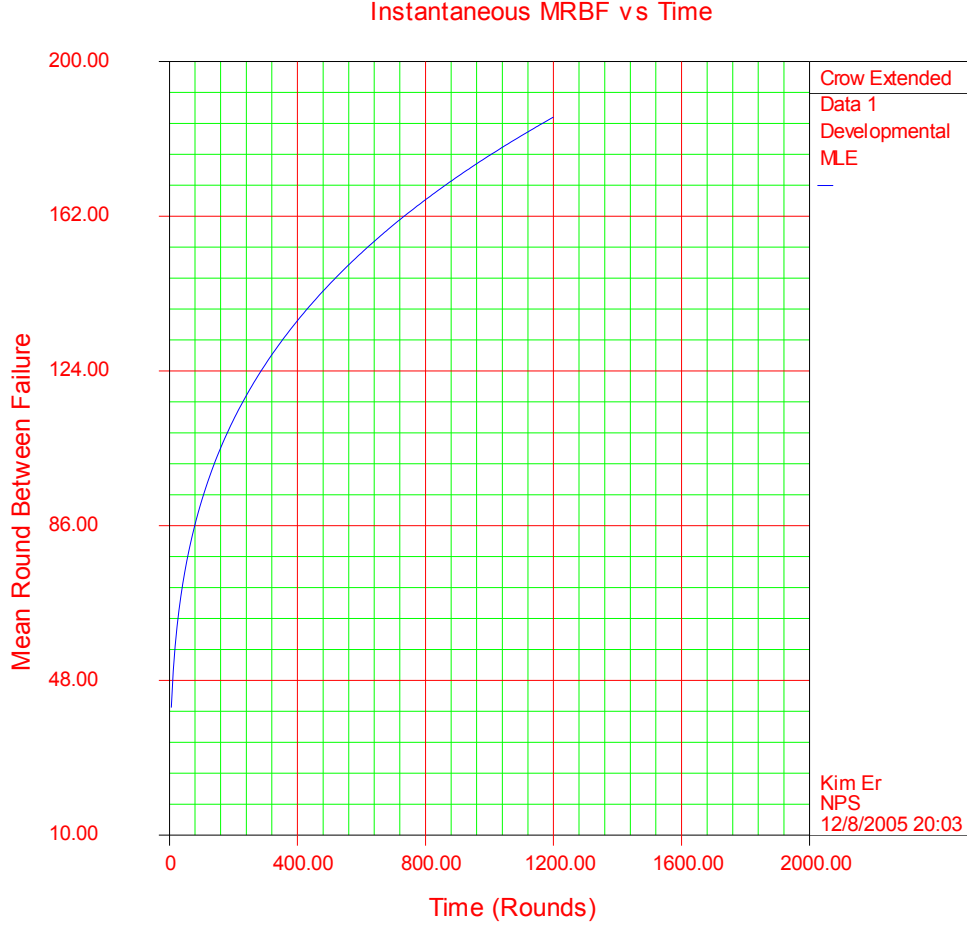


Figure 13. MRBF vs time plot for Phase 3

The projected failure intensity after the incorporation of delay fixes into the system is calculated using equation 4.16.

$$\hat{\lambda}_{EM} = \hat{\lambda}_{CA} - \hat{\lambda}_{BD} + \sum_{j=1}^M (1 - d_j) \frac{N_j}{T} + \bar{d} \hat{h}(T / BD)$$

The failure intensity for Type BD failure modes is given by

$$\hat{\lambda}_{BD} = \frac{\text{Total number of Type BD failure modes}}{\text{Total test time}} = \frac{3}{1200} = 0.0025$$

The term $\hat{h}(T / BD) = \hat{\lambda} \hat{\beta} T^{\beta-1}$ from equation 4.14 is a function of $\hat{\beta}$ and $\hat{\lambda}$. These two parameters are estimated from equations 4.5 and 4.6 using first occurrence data from Table 17.

$$\hat{\beta} = \frac{N}{N \ln T - \sum_{i=1}^N \ln X_i} = \frac{3}{\left[3 \ln 1200 - (\ln 55 + \ln 520 + \ln 579) \right]} = 0.645$$

The growth rate due to the three distinct fixes is given by equation 4.3

$$\alpha_{DUANE} = 1 - \beta_{AMSAA} = 1 - 0.645 = 0.355$$

$$\hat{\lambda} = \frac{N}{T^{\hat{\beta}}} = \frac{3}{1200^{0.645}} = 0.0309 \text{ failures/round}$$

$$\hat{h}(T / BD) = \hat{\lambda} \hat{\beta} T^{\beta-1} = 0.001615$$

This metric $\hat{h}(T / BD)$ represents the intensity for Type BD failure modes that have not been seen during the testing which also means the rate at which new distinct Type BD modes are occurring at the end of the test.

The average EF is given by equation 4.13

$$\bar{d} = \text{Average EF} = \frac{\sum_{j=1}^M d_j}{M} = \frac{0.6 + 0.6 + 0.6}{3} = 0.6$$

Finally, the projected failure intensity after the incorporation of delayed fixes into the system for the Extended Model can be determined as

$$\begin{aligned} \hat{\lambda}_{EM} &= \hat{\lambda}_{CA} - \hat{\lambda}_{BD} + \sum_{j=1}^M (1 - d_j) \frac{N_j}{T} + \bar{d} \hat{h}(T / BD) \\ &= 0.00533 - 0.0025 + \sum_{j=1}^3 (1 - d_j) \frac{N_j}{1200} + 0.6 * 0.001615 \\ &= 0.00483 \end{aligned}$$

The Extended Model projected MRBF after the incorporation of delay fixes at the end of the test is given by equation 4.17.

$$\hat{M}_{EM} = \frac{1}{\hat{\lambda}_{EM}} = 206.7$$

For a two-sided confidence level of 90 %, the projected MRBF is between 105 and 404 rounds.

A sensitivity analysis on the effects of varying EF on MRBF was carried out and the results shows that the projected MRBF increases to 220 rounds or by 7 percent if the assumed EF is 0.9. It can therefore be concluded that the resulting MRBF does not vary significantly when using two extreme values of EF.

Analysis Results				
β :	0.6455		PMTBF:	206.7
$\hat{\lambda}$:	0.0309			
Statistical Results				
	Result		Test Value	Upper
Cram'er Von Mises (BD)	Passed		0.0872	0.154

Table 19. RGA 6 PRO BD failure modes analysis results and Cramer Von Mises statistical test results for Phase 3

The RGA 6 PRO generated results presented in Table 19 are consistent with the hand calculated values. The Cramer-Von Mises statistics of 0.0872 is below the critical value of 0.154 for a significance level of 0.1. Hence the hypothesis that the AMSAA model is appropriate is accepted.

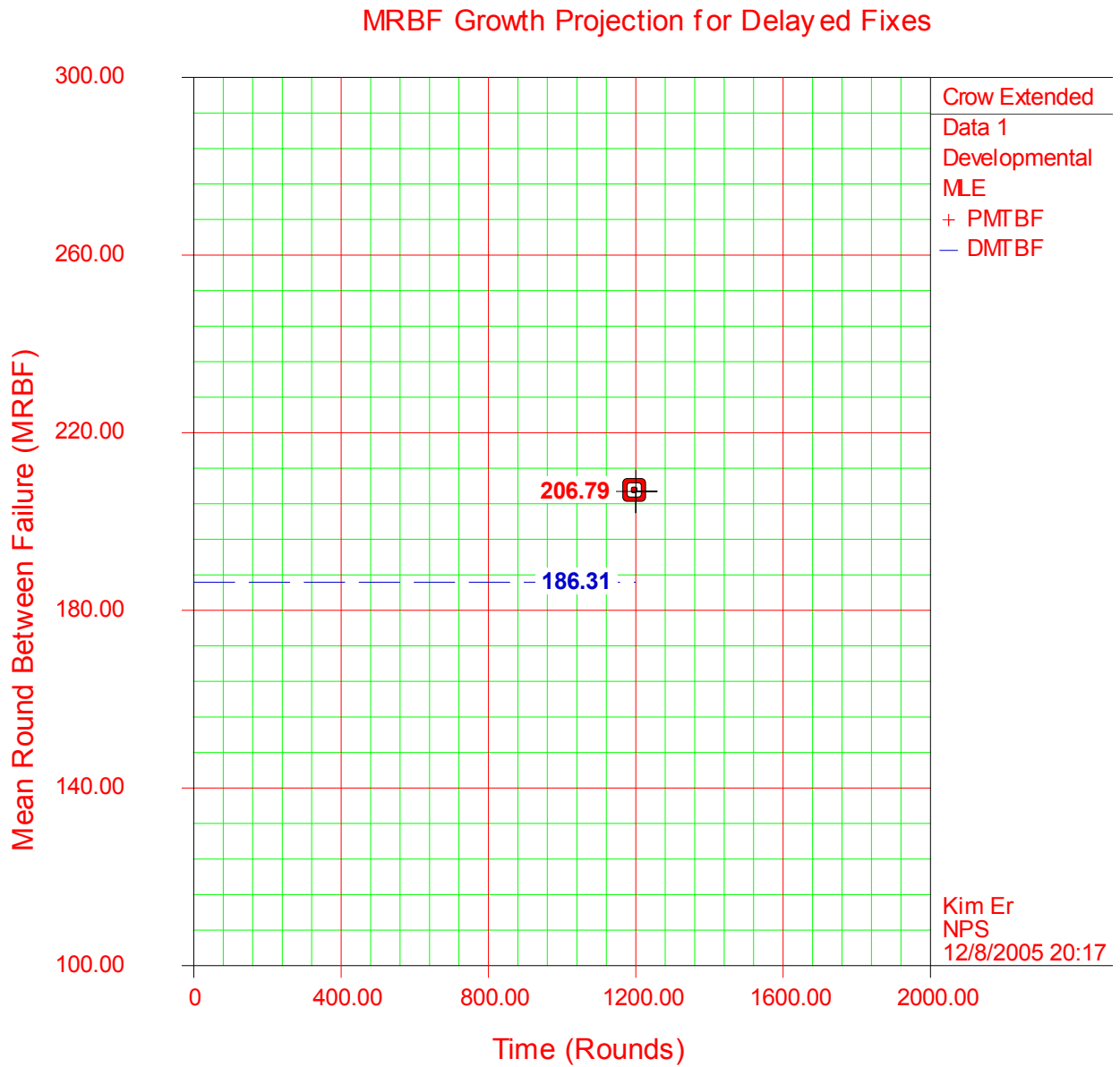


Figure 14. Projected MRBF vs time plot for Phase 3

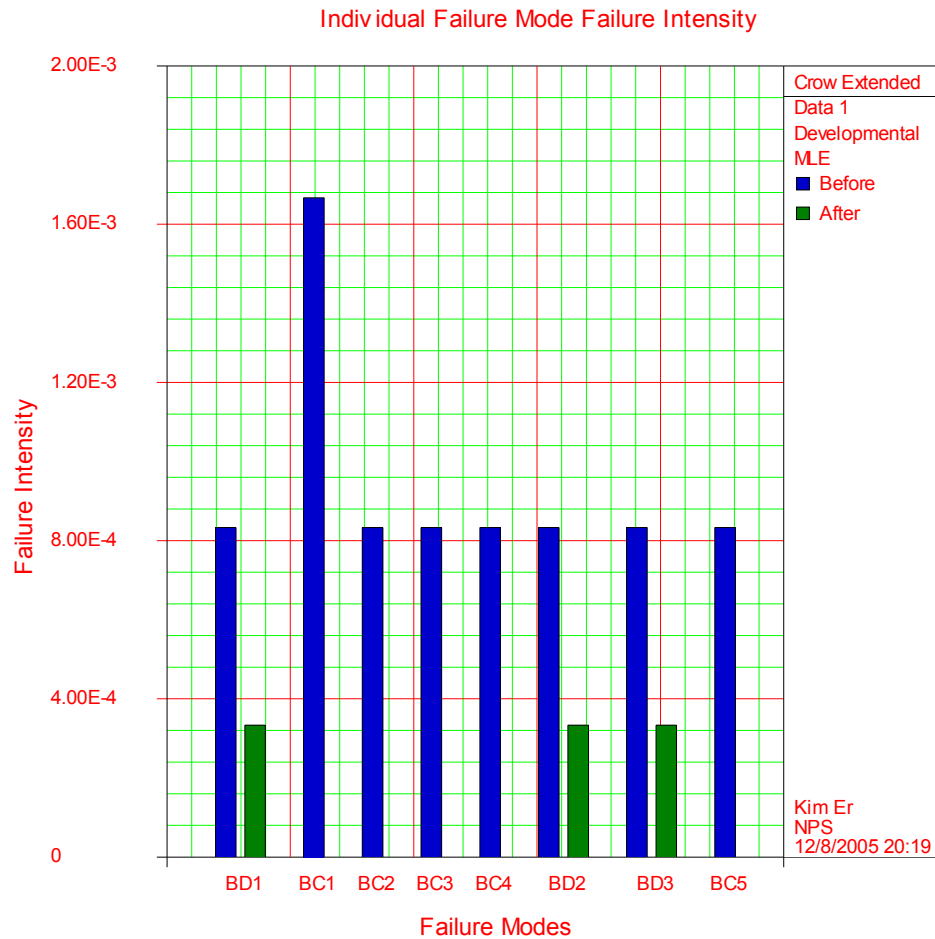


Figure 15. Individual failure rate of Type BC and BD failure modes at the end of Phase 3

The Extended Model estimates that the MRBF grew to 186 rounds as a result of three corrective actions for BC failure modes during the test. It then jumps to 206.7 rounds as a result of the delayed corrective actions for the Type BD failure modes even with conservative EF estimates of 0.6. The system is estimated to meet the reliability requirements after taking into account the effect of delayed fixes. To provide additional insights, Figure 15 shows the individual failure rate contribution of both Type BC and Type BD failure modes. In comparison, failure mode Type BC1 has the highest relative failure rate. On the other hand, the failure rates of Type BD1, BD2 and BD3 has decreased significantly after fixing. To substantiate this claim from an engineering viewpoint, the fixes for these three BD modes involves only basic component replacement or repair. The assigned EF of 0.6 is a conservative estimate for simple fixes and hence it can be concluded that the projected MRBF of 206 rounds is a realistic

estimate. In order for the reliability of the system to grow further, efforts should be focused on improving the correction action for failure mode BC1 despite the last corrective action has proven to be effective.

The system grows from an initial demonstrated MRBF of 93 rounds to 206 rounds. In conclusion, the system is estimated to meet the reliability requirements at the end of the RGT. However, the projected MRBF falls between 105 and 404 rounds for a two-sided confidence level of 90 %,

D. RELIABILITY GROWTH ANALYSIS FOR SUBSYSTEM B

Reliability growth for subsystem B is tracked over three phases of testing. Reliability is tracked on a phase by phase basis. Similarly, data collected during each phase is analyzed using the ReliaSoft's RGA 6 PRO software [Ref. 21]. The reliability growth model selected for reliability analysis for the three test phases is:

Phase 1: AMSAA Extended Test-Find-Test Projection Model

Phase 2: AMSAA Extended Test-Fix-Test Model

Phase 3: AMSAA Extended Test-Fix-Test Model

1. Phase 1 results and analysis

In Phase 1, the prototype system was subjected to 1000 kilometers of testing. During the test five failures were identified but all corrective actions were delayed till the end of the test. This management strategy is known as test-find-test. The AMSAA Extended Test-Find-Test Model is selected to analyze the reliability of the system after the incorporation of delayed fixes. The failures identified during the test were classified into their respective failure category as shown in Table 20.

j	Time to Event, X_j	Classification	Mode	Failure Category
1	159	BD	1	Workmanship
2	252	BD	2	Quality
3	299	BD	3	Design
4	555	BD	3	Design
5	967	BD	4	Quality

Table 20. Test-find-test data for Phase 1

BD Mode	Number of Failures, N_j	Time to First Occurrence	EF, d_j
1	1	159	0.7
2	1	252	0.7
3	2	299	0.6
4	1	967	0.7

Table 21. Test-find-test Type B failure mode data and effectiveness factor for Phase 1

There is no Type A failure modes since all failures will received corrective actions. There are five unique modes of Type B failure. All Type B failure modes are classified as BD. The EF for each BD failure mode assigned in Table 21 is based on engineering assessment on the level of effectiveness of the corrective action.

The achieved system failure intensity is only contributed to by Type B failure mode which is estimated by equation 4.8:

$$\hat{\lambda}_s = \hat{\lambda}_{BD} = \frac{N_B}{T} = \frac{5}{1000} = 0.005$$

The estimated achieved MKBF at T=1000 kilometers before the jump is

$$\hat{M}_s = \frac{1}{\hat{\lambda}_s} = 200 \text{ kilometers}$$

Next, the projected failure intensity is calculated is calculated using equation 4.12.

$$\hat{\lambda}_p = \hat{\lambda}_A + \sum_{j=1}^M (1 - d_j) \frac{N_j}{T} + \bar{d}\hat{h}(T)$$

The average EF of the delay fixes is given by equation 4.13

$$\bar{d} = \text{Average EF} = \frac{\sum_{j=1}^M d_j}{M} = \frac{0.7 + 0.7 + 0.6 + 0.7}{4} = 0.675$$

The term $\hat{h}(T / BD) = \hat{\lambda}\hat{\beta}T^{\beta-1}$ from equation 4.14 is a function of $\hat{\beta}$ and $\hat{\lambda}$. These two parameters are estimated from equations 4.5 and 4.6 using first occurrence data from Table 21.

$$\hat{\beta} = \frac{N}{N \ln T - \sum_{i=1}^N \ln X_i} = \frac{4}{[4 \ln 1000 - (\ln 159 + \ln 252 + \ln 299 + \ln 967)]}$$

$$= 0.8973.$$

$$\hat{\lambda} = \frac{N}{T^{\hat{\beta}}} = \frac{4}{1000^{0.8973}} = 0.00813 \text{ failures/kilometers}$$

$$\hat{h}(T / BD) = \hat{\lambda} \hat{\beta} T^{\hat{\beta}-1} = 0.00358$$

This metric $\hat{h}(T / BD)$ represents the intensity for Type BD failure modes that have not been seen during the testing which also means the rate at which new distinct Type BD modes are occurring at the end of the test

With all the above parameters defined, the projected failure intensity can be calculated.

$$\hat{\lambda}_p = \hat{\lambda}_A + \sum_{j=1}^M (1 - d_j) \frac{N_j}{T} + \bar{d} \hat{h}(T) = \sum_{j=1}^4 (1 - d_j) \frac{N_j}{1000} + 0.675 * 0.00358 = 0.00411$$

The projected MRBF due to the jump is the inverse of the projected failure intensity given by equation 4.15.

$$\hat{M}_p = \frac{1}{\hat{\lambda}_p} = 242 \text{ kilometers}$$

For a two-sided confidence level of 90%, the projected MKBF is between 103 and 829 kilometers.

A sensitivity analysis on the effects of varying EF on MKBF was carried out and the results show a 10 percent difference if the EF is varied from 0.6 to 0.9. It can therefore be concluded that although MKBF increases with an increasing value of EF but using two extreme values of EF does not produce very significant difference in the MKBF.

Projection Summary				
β :	0.8973		PMTBF:	242.56
$\hat{\lambda}$:	0.00813		DMTBF:	200
Statistical Results				
	Result		Test Value	Upper
Cram'er Von Mises (BD)	Passed		0.0919	0.155

Table 22. RGA 6 PRO projection summary and Cramer Von Mises test results for Phase 1

The RGA 6 PRO generated results as shown in Table 22 is similar to the hand calculated values. The Cramer-Von Mises statistics of 0.0919 is below the critical value of 0.155 for a significance level of 0.1. Hence the hypothesis that the AMSAA model is appropriate is accepted. From Table 22, it can be seen that the $\hat{\beta}$ value of subsystem B is higher than subsystem A which implies a lower growth rate. This is expected because subsystem B is an OTS system.

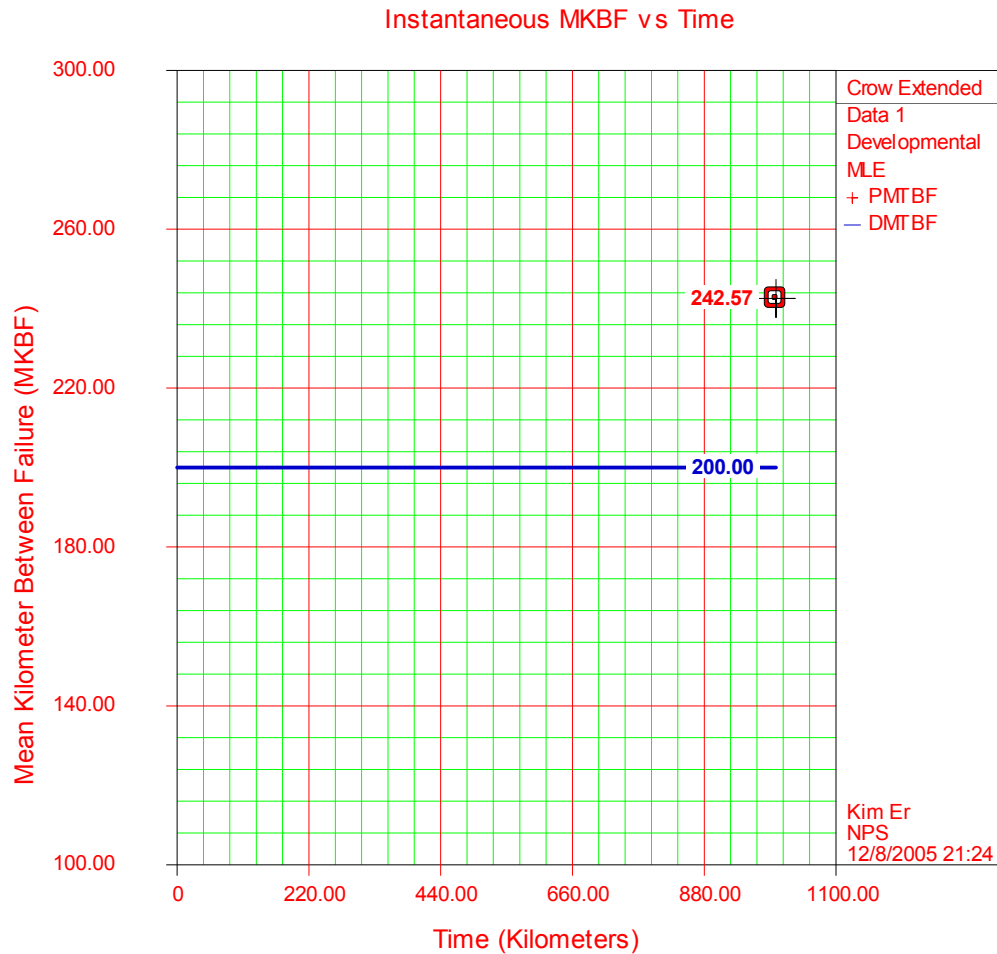


Figure 16. MKBF projection for Phase 1

Figure 16 shows the plot of reliability versus time for subsystem B during the test. The reliability of subsystem B is constant ($\beta = 1$) during the test because no fixes were implemented on the system and therefore no growth is taking place during the test. There is a jump in reliability at the end of the test due to fixes being incorporated into the system. The projection model estimates that the MKBF jumps to 242 kilometers at the end of phase 1 due to four distinct corrective actions in redesign and quality process and workmanship improvement. This projected MKBF value of 242 has exceeded the planned MKBF of 229 kilometers which concludes that reliability growth is progressing satisfactorily at the end of phase 1.

The failure trend in Figure 17 shows that majority of the failures were surfaced during the early stages of the testing which is typical of a new system during its initial run-in. These are infant mortality failures due to poor quality and workmanship of components.

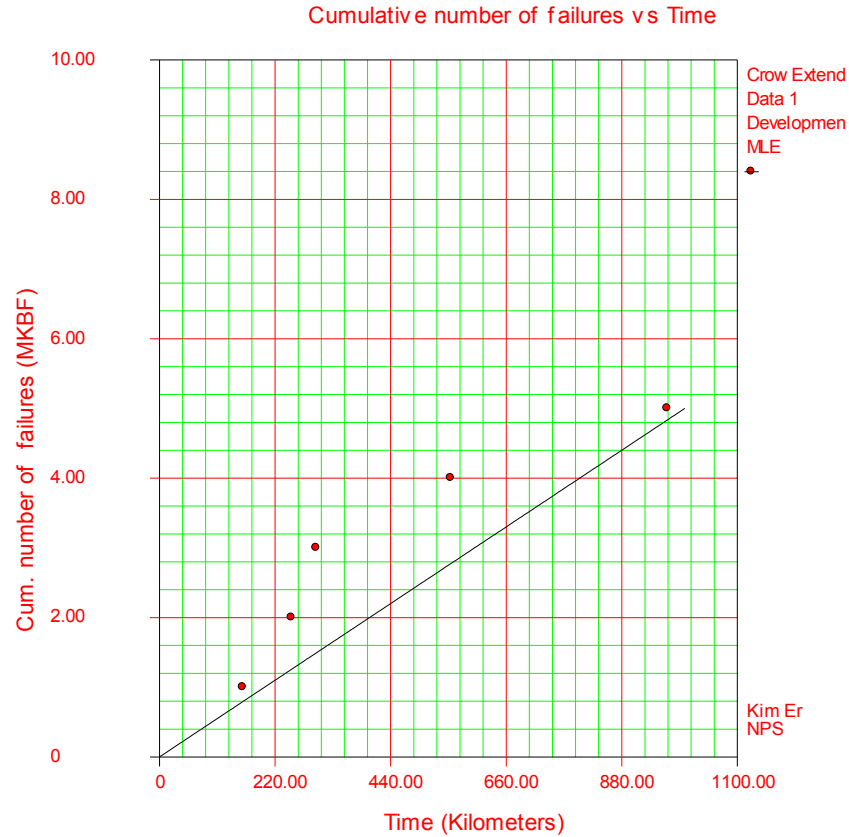


Figure 17. Cumulative number of failures vs time plot for Phase 1

In addition, the fraction of seen and unseen Type BD failure intensity can also be estimated. The intensity for Type BD failure modes that have been seen in the testing can be estimated as follows:

$$\hat{\lambda}_{BD} - \hat{h}(1000 / BD) = 0.005 - 0.00358 = 0.00142$$

The fraction of Type BD failure intensity due to failure modes that have been seen in test is:

$$\text{Fraction Seen} = \frac{\hat{h}(1000 / BD)}{\hat{\lambda}_{BD}} = 0.284$$

$$\text{Fraction Unseen} = 0.716$$

Figure 18 displays the failure rate for each individual Type BD failure modes before and after implementing the fixes. It provides a clear visibility on the failure rate contribution of each individual Type BD failure mode to the system's overall failure rate. The failure management strategy should focus on fixing mode BD3 as it appears to have the highest failure rate from Figure 17.

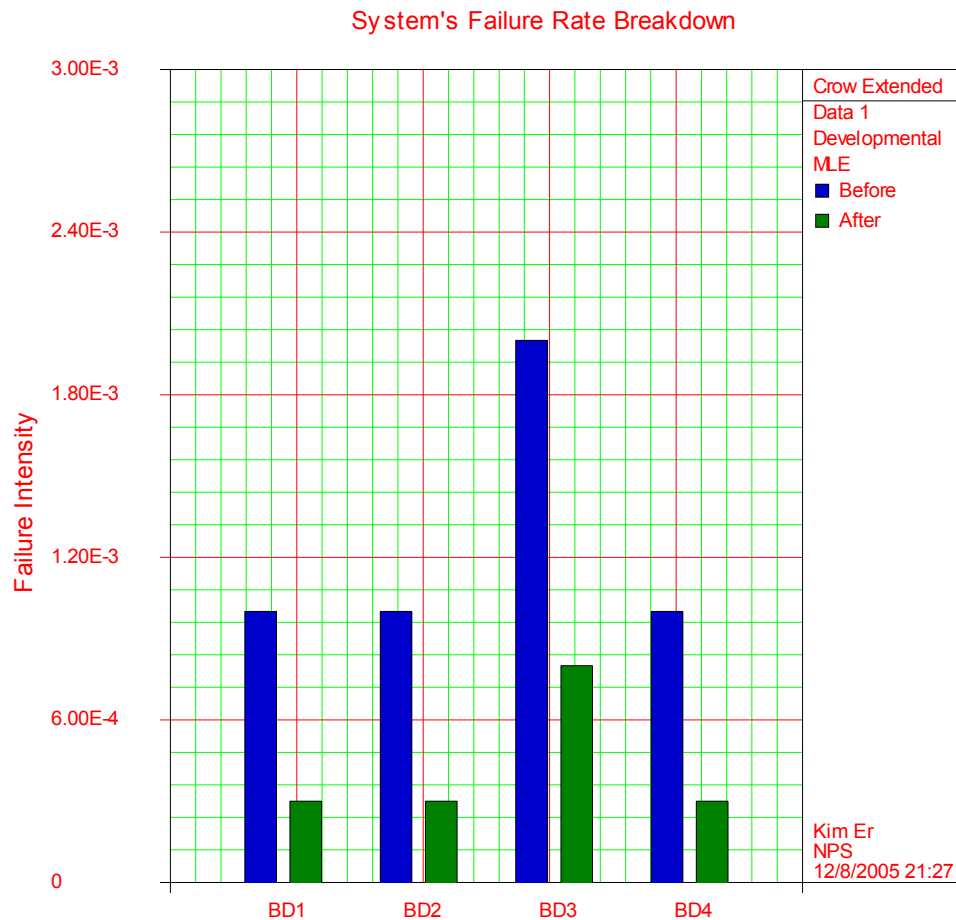


Figure 18. Before and after failure rate for Type BD failure mode in Phase 1

2. Phase 2 results and analysis

The testing approach used in Phase 2 is Test-Analyze-And-Fix (TAAF), in which fixes for all failure modes discovered are being incorporated during the test. The total cumulative test mileage for this phase is 1600 kilometers. The AMSAA Extended Test-

Fix-Test Model is used to analyze the reliability for this phase. All failure modes are being classified under Type BC in Table 23.

j	Time to Event, X_j	Classification	Mode	Failure Category
1	89	BC	1	Design
2	147	BC	2	Faulty Component
3	356	BC	3	Design
4	626.84	BC	4	Quality
5	719	BC	3	Quality
6	1285.4	BC	5	Design
7	1420	BC	6	Design

Table 23. Test-fix-test data for Phase 2

BC Mode	Number of Failures, N_j	Time to First Occurrence
1	1	89
2	1	147
3	2	434.6
4	1	626.84
5	1	1285.4
6	1	1420

Table 24. Unique first time occurrence BC failure mode for Phase 2

During this phase, six unique failures were observed in 1600 kilometers of testing. With the above test data, the demonstrated MKBF for this test phase can be calculated.

The shape parameter is estimated using equation 4.5.

$$\begin{aligned}
 \hat{\beta} &= \frac{N}{N \ln T - \sum_{i=1}^N \ln X_i} \\
 &= \frac{7}{\left[6 \ln 1600 - (\ln 89 + \ln 147 + \ln 434.6 + \ln 626.8 + \ln 719 + \ln 1285.4 + \ln 1420) \right]} \\
 &= 0.7905
 \end{aligned}$$

The calculated $\hat{\beta}$ of 0.7905 ($\hat{\beta} < 1$) is lower than Phase 1 which implies reliability improvement compared to the last phase.

The relationship between the growth rate and the shape parameter is given by equation 4.2.

$$\alpha_{DUANE} = 1 - \beta_{AMSAA} = 1 - 0.7905 = 0.2095$$

The scale parameter is estimated using equation 4.6.

$$\hat{\lambda} = \frac{N}{T^{\hat{\beta}}} = \frac{7}{1600^{0.7905}} = 0.0205$$

The achieved failure intensity at the end of the test is estimated by equation 4.3.

$$\hat{\lambda}_{CA} = r(T) = \hat{\lambda} \hat{\beta} T^{\hat{\beta}-1} = 0.0205 * 0.7905 * 1600^{0.7905-1} = 0.00345$$

The demonstrated instantaneous MKBF at the end of phase 2 after 1600 kilometers of testing is given in equation 4.4.as the reciprocal of the intensity function:

$$\hat{M}_{CA} = \frac{1}{\lambda_{CA}} = 289 \text{ kilometers}$$

For a two-sided confidence level of 90 %, the demonstrated MKBF is between 119 and 953 kilometers.

Another useful metric is the initial system instantaneous MKBF at the beginning of this phase. It is given in equation 4.21.

$$M_I = \frac{\Gamma\left(1 + \frac{1}{\hat{\beta}}\right)}{\hat{\lambda}^{\frac{1}{\hat{\beta}}}} = 156 \text{ kilometers} \quad (4.22)$$

The initial MRBF of 156 kilometers at the beginning of Phase 2 is within the confidence interval of 110 and 534 kilometers at the end of Phase 1. At the beginning of the test it is estimated that the initial system MKBF was 156 kilometers and due to six distinct fixes the reliability grew to 289 kilometers at the end of 1600 kilometers of testing.

Analysis Summary				
Model:	Crow-AMSAA (NHPP)		Analysis Method:	MLE
$\hat{\beta}$:	0.7905		Test Procedure:	Developmental
$\hat{\lambda}$:	0.0205		Input Type:	Cumulative
Growth Rate:	0.2095		Termination Time:	1600
Instant. MTBF:	289.13			
Statistical Results				
	Result		Test Value	Upper
Cram'er Von Mises	Passed		0.0275	0.165

Table 25. RGA 6 PRO analysis summary and Cramer Von Mises test results for Phase 2

The RGA 6 PRO generated results are presented in Table 25. The Cramer-Von Mises statistics of 0.0275 is below the critical value of 0.165 for a significance level of 0.1. Hence the hypothesis that the AMSAA model is appropriate is accepted.

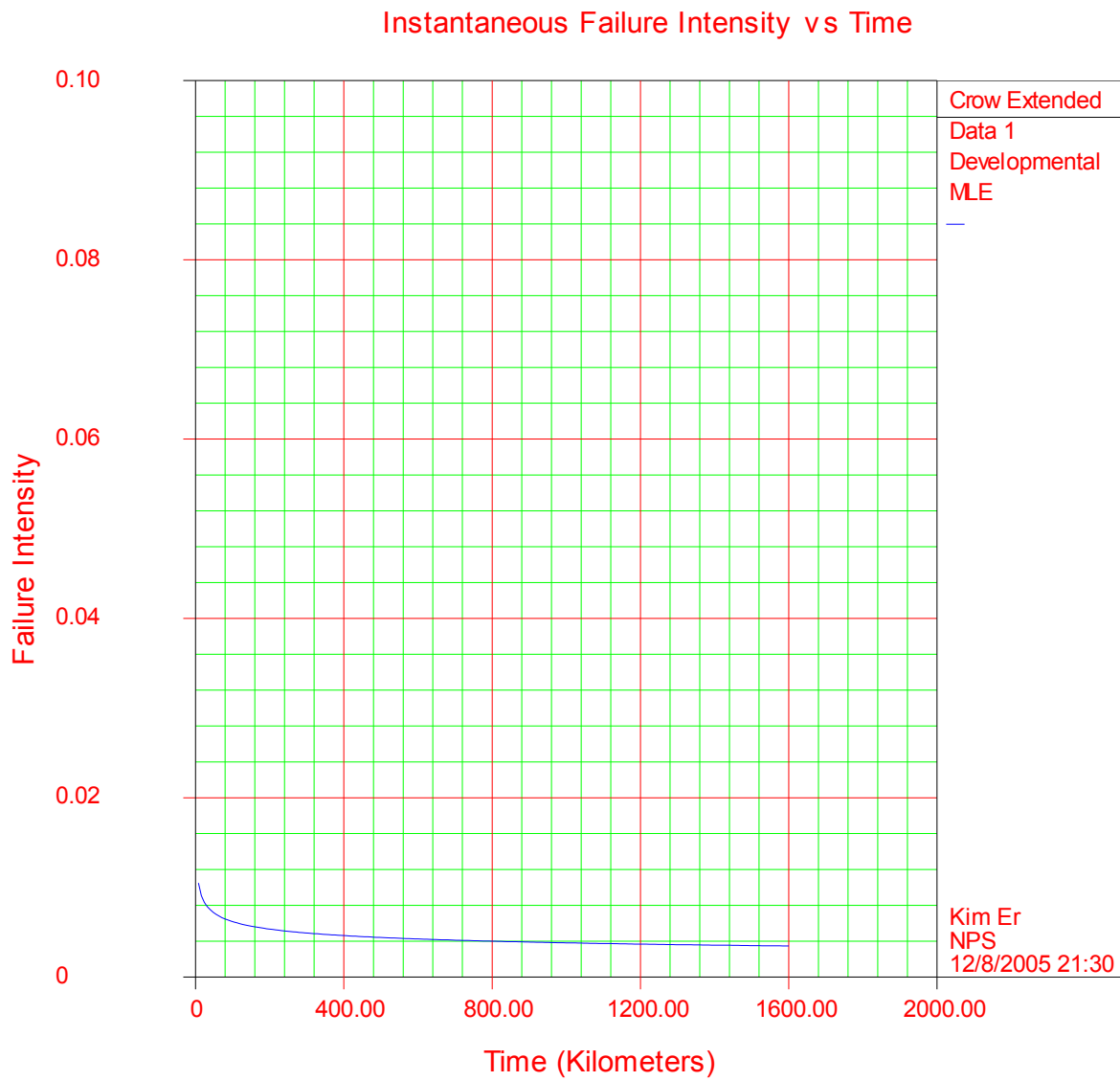


Figure 19. Failure intensity vs time plot for Phase 2

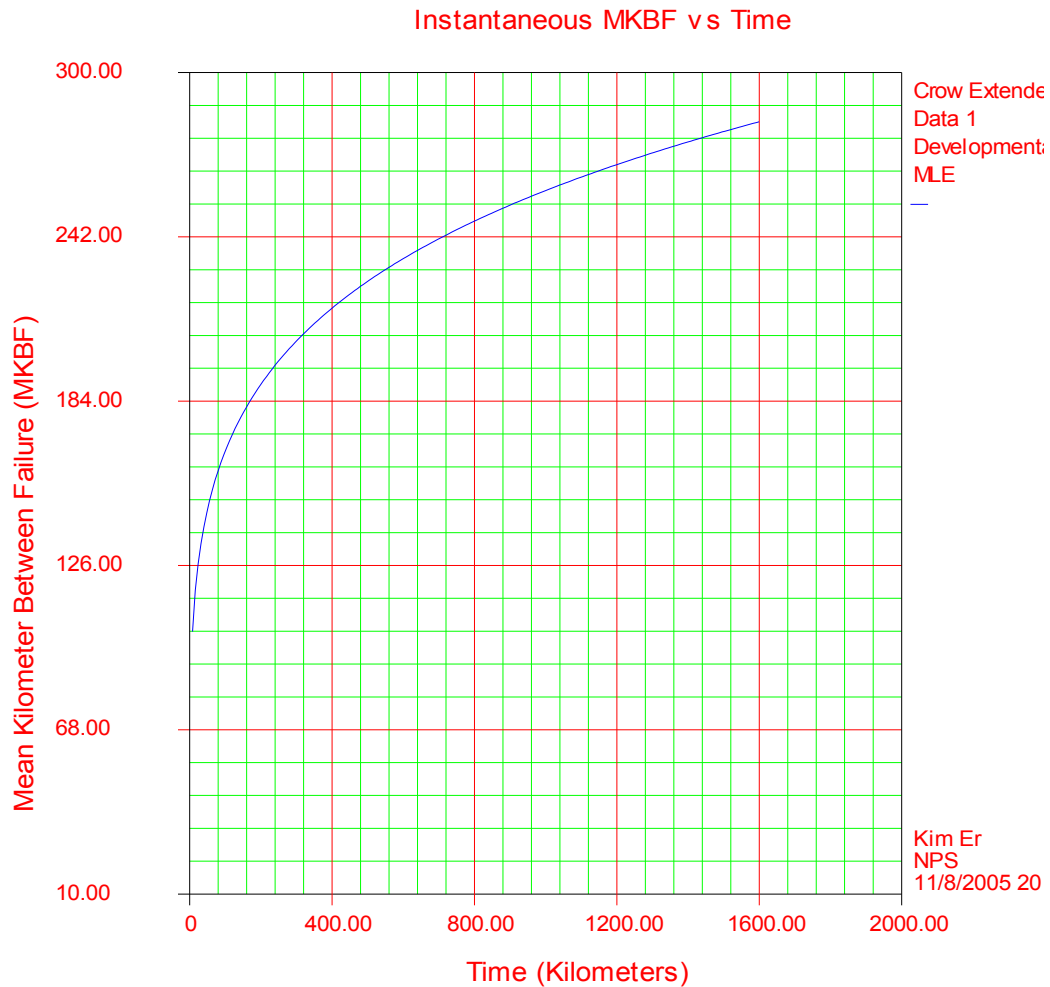


Figure 20. MKBF vs time plot for Phase 2

According to the idealized growth curve, the expected MKBF at the end of phase 2 should be approaching 296 kilometers. It is obvious from the instantaneous failure intensity versus time plot in Figure 19 that the decrease in the failure intensity is not significant throughout the test. Clearly, the main reason is due to the high frequency of occurrence of failure mode BC3 as display in Figure 21. At this point the program manager must focus on correcting this failure mode.

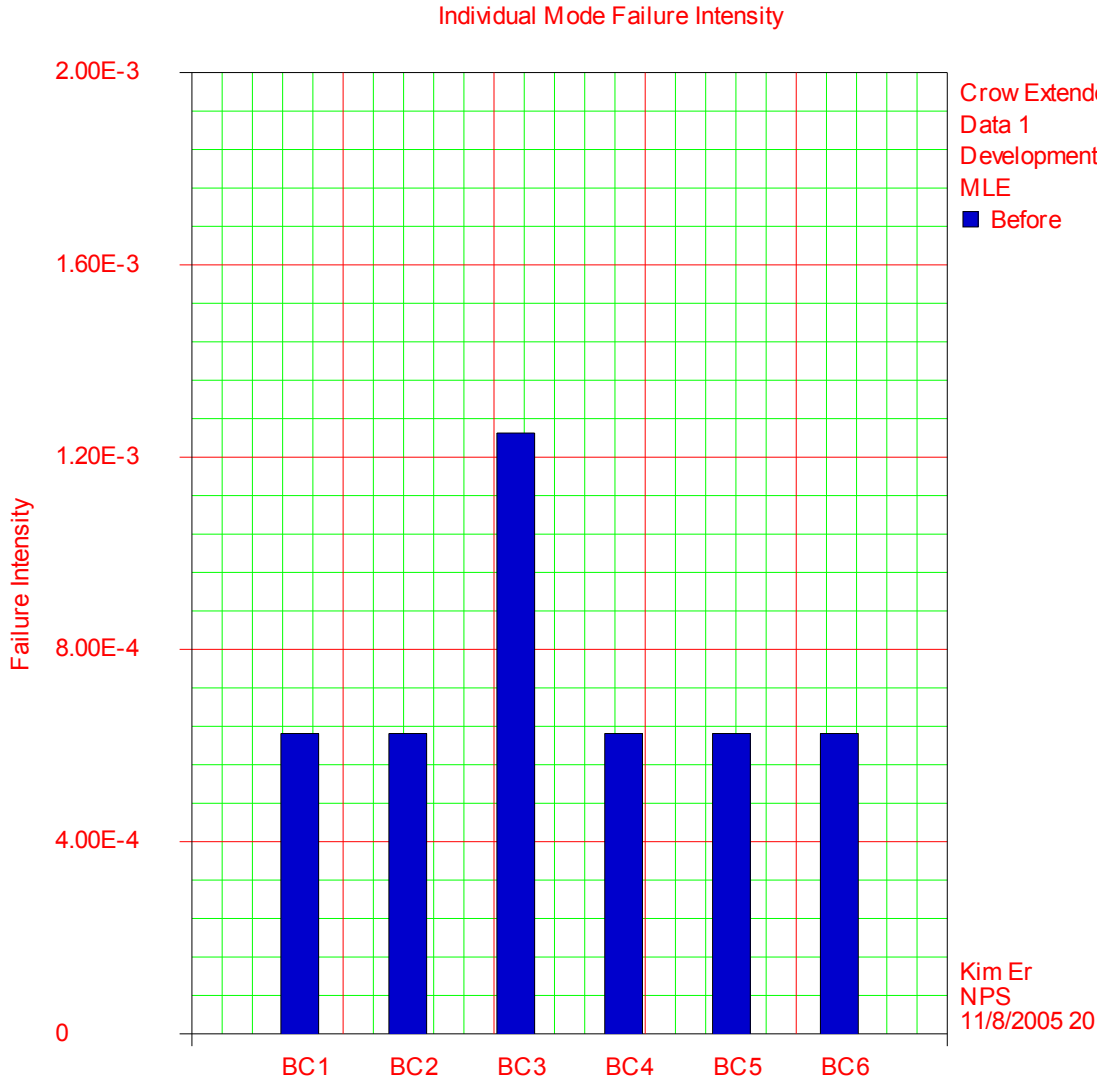


Figure 21. Failure rate of individual BC failure modes at the end of test

Lastly, it may also be of interest from an engineering perspective to estimate the level of effectiveness of the fixes for the six Type BC failure modes. The average effectiveness factor can be calculated as follows [Ref.20]:

$$\hat{d}_{BC} = \frac{\hat{\lambda}_I - \hat{\lambda}_{CA}}{\hat{\lambda}_{I(BC)} - \hat{h}(T / BC)} \quad (4.23)$$

The initial system failure intensity is the inverse of the initial system MRBF in equation 4.22.

$$\lambda_I = \lambda_{BC} = \frac{1}{M_I} = \frac{1}{156} = 0.00641$$

Since there are no Type A failure mode in the data, the initial failure intensity for Type BC failure modes is equals to the initial failure intensity of the system.

λ_{CA} is the achieved system failure intensity at the end of the test phase which has been determined. Next is to determine the failure intensity for new Type BC failure modes at the end of this test phase. This is the same as equation 4.14 but considers only BC modes.

$$\hat{h}(T / BC) = \hat{\lambda} \hat{\beta} T^{\hat{\beta}-1}$$

The estimate of $\hat{\lambda}$ and $\hat{\beta}$ is calculated using equations 4. 5 and 4.6 based on the first time occurrence data for BC failure modes in Table 23.

$$\begin{aligned} \hat{\beta} &= \frac{N}{N \ln T - \sum_{i=1}^N \ln X_i} \\ &= \frac{6}{\left[6 \ln 1200 - (\ln 89 + \ln 147 + \ln 434.6 + \ln 626.8 + \ln 1285 + \ln 1420) \right]} \\ &= 0.763 \end{aligned}$$

$$\hat{\lambda} = \frac{N}{T^{\hat{\beta}}} = \frac{6}{1200^{0.763}} = 0.0214$$

$$\hat{h}(T / BC) = \hat{\lambda} \hat{\beta} T^{\hat{\beta}-1} = 0.00304$$

Finally the average EF for Type BC failure modes can be determined

$$\hat{d}_{BC} = \frac{\hat{\lambda}_I - \hat{\lambda}_{CA}}{\hat{\lambda}_{I(BC)} - \hat{h}(T / BC)} = 0.878 \quad (4.24)$$

In conclusion, the six corrective actions remove an average of 87.8 % of the failure rate from the six unique failure modes. An average of 12.2 % remained in the six BC modes. The average EF of 0.87 is high which implies that the corrective actions that have been incorporated are very effective.

3. Phase 3 results and analysis

The TAAF approach should be applied in the last test phase so that the effectiveness of all corrective actions implemented during the test can be verified by the end of the test. Hence a more accurate assessment of the system reliability based on the current configuration can be obtained. In Phase 3, all fixes are incorporated during the test. The system was tested for 2250 kilometers in this phase. During this phase the MKBF of the system was continuously assessed to provide constant technical and management visibility on the effectiveness of corrective actions and program status.

Testing was terminated prematurely at 2200 kilometers instead of the planned 2250 kilometers because the system reliability has exceeded the requirement. The data collected during the test is presented in Table 26.

j	Time to Event, X_j	Classification	Mode	Failure Category
1	36	BC	1	Design
2	334	BC	2	Quality
3	823.6	BC	3	Faulty component
4	958	BC	4	Workmanship
5	960	BC	5	Faulty component
6	1433	BC	6	Quality
7	1741	BC	7	Workmanship

Table 26. Test-fix-test data for Phase 3

The AMSAA Extended Test-Fix-Test Model is used to analyze the test data in Table 26.

The shape parameter is estimated using equation 4.5

$$\begin{aligned}
 \hat{\beta} &= \frac{N}{N \ln T - \sum_{i=1}^N \ln X_i} \\
 &= \frac{7}{\left[7 \ln 2200 - (\ln 36 + \ln 334 + \ln 823.6 + \ln 958 + \ln 960 + \ln 1433 + \ln 1741) \right]} \\
 &= 0.7524
 \end{aligned}$$

The scale parameter is estimated using equation 4.6

$$\hat{\lambda} = \frac{N}{T^{\hat{\beta}}} = \frac{7}{2200^{0.7524}} = 0.0214$$

The relationship between the growth rate and the shape parameter is given by equation 4.2.

$$\alpha_{DUANE} = 1 - \beta_{AMSA} = 0.25$$

The growth rate of 0.25 indicates a significant improvement compared to Phase 2.

The achieved failure intensity is estimated as:

$$\hat{\lambda}_{CA} = r(T) = \hat{\lambda} \hat{\beta} T^{\hat{\beta}-1} = 0.0214 * 0.7524 * 2200^{0.7524-1} = 0.00239$$

The demonstrated instantaneous MKBF at the end of the test phase after 2200 kilometers of testing is given in equation 4.4 as the reciprocal of the intensity function:

$$\hat{M}_{CA} = \frac{1}{\lambda_{CA}} = 417 \text{ kilometers}$$

For a confidence interval of 90 %, the projected MKBF falls between 172 and 1377 kilometers.

Another useful metric is the initial system MKBF at the beginning of this phase. It is given by equation 4.21.

$$M_I = \frac{\Gamma\left(1 + \frac{1}{\hat{\beta}}\right)}{\hat{\lambda}^{\frac{1}{\hat{\beta}}}} = 197 \text{ kilometers}$$

The initial MRBF of 197 kilometers at the beginning of Phase 3 is within the confidence interval of 103 and 829 kilometers at the end of Phase 2. At the beginning of the test it is estimated that the initial system MKBF was 197 kilometers and due to seven distinct fixes the reliability grew to 417 kilometers at the end of 2200 kilometers of test.

Model:	Crow-AMSAA (NHPP)		Analysis Method:	MLE
β :	0.7524		Test Procedure:	Developmental
λ :	0.0214		Input Type:	Cumulative
Growth Rate:	0.2476		Termination Time:	2200
Instant. MTBF:	417.71			
Statistical Results				
	Result		Test Value	Upper
Cram'er Von Mises	Passed		0.0647	0.165

Table 27. RGA 6 PRO analysis summary and Cramer Von Mises test results for Phase 3

The RGA Pro 6 generated summary and statistical results are presented in Table 27. The Cramer-Von Mises statistics of 0.0647 is below the critical value of 0.165 for a significance level of 0.1. Hence the hypothesis that the AMSAA model is applicable is accepted.

The AMSAA Test-Fix-Test Model estimates that the demonstrated MKBF of 417 kilometers at the end of 2200 kilometers of testing has exceed the requirement of 350 kilometers. The test was terminated at a cumulative mileage 2200 kilometers primarily for two reasons: 1) It can be observed from the cumulative number of failures versus time plot in Figure 22 that there is a decreasing trend in the number of observed failures towards the end of the test and 2) the MKBF requirement has already been exceeded. There are only two failures observed in the last 1100 kilometers of testing. The achieved growth rate of 0.25 is also a significant improvement compared to Phase 2. The effectiveness of the fixes in previous phases have been validated which represents an obvious reason for the improved reliability. Also, the $\hat{\beta}$ value of subsystem B is higher as than subsystem A in all three phases of testing which implies a lower growth rate. This is expected because subsystem B is an OTS system.

In conclusion, the implementation of the TAAF approach for subsystem B has been successful in surfacing and fixing potential failure modes and thus exceeding the reliability target. The system grows from an initial demonstrated MKBF of 200

kilometers to 417 kilometers. The RGT program has identified reviewed and fixed a total of four unique design failure modes and six quality process and control failure modes during the three phases of testing leading to positive reliability growth.

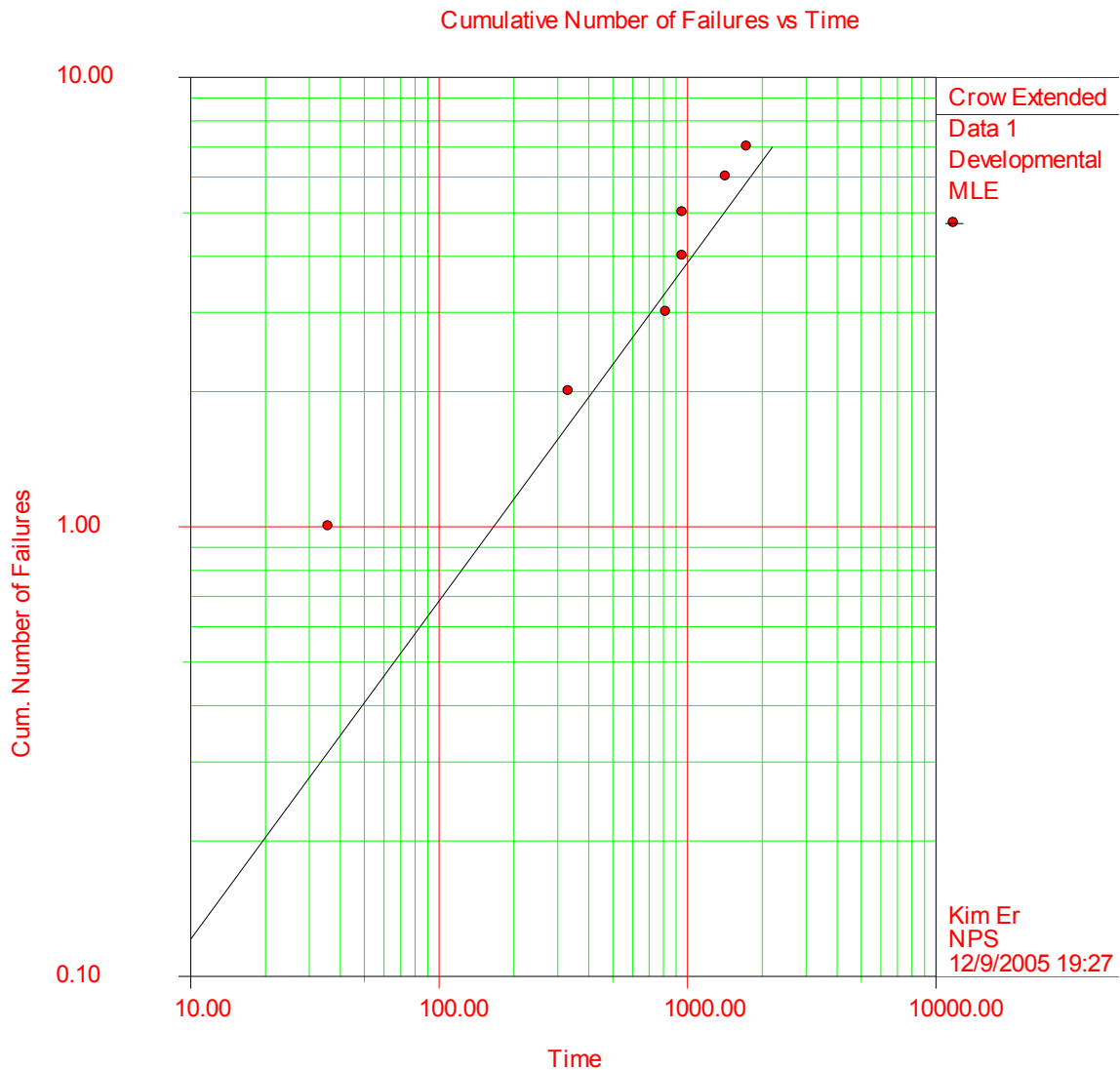


Figure 22. Cumulative number of failures vs time plot for Phase 3

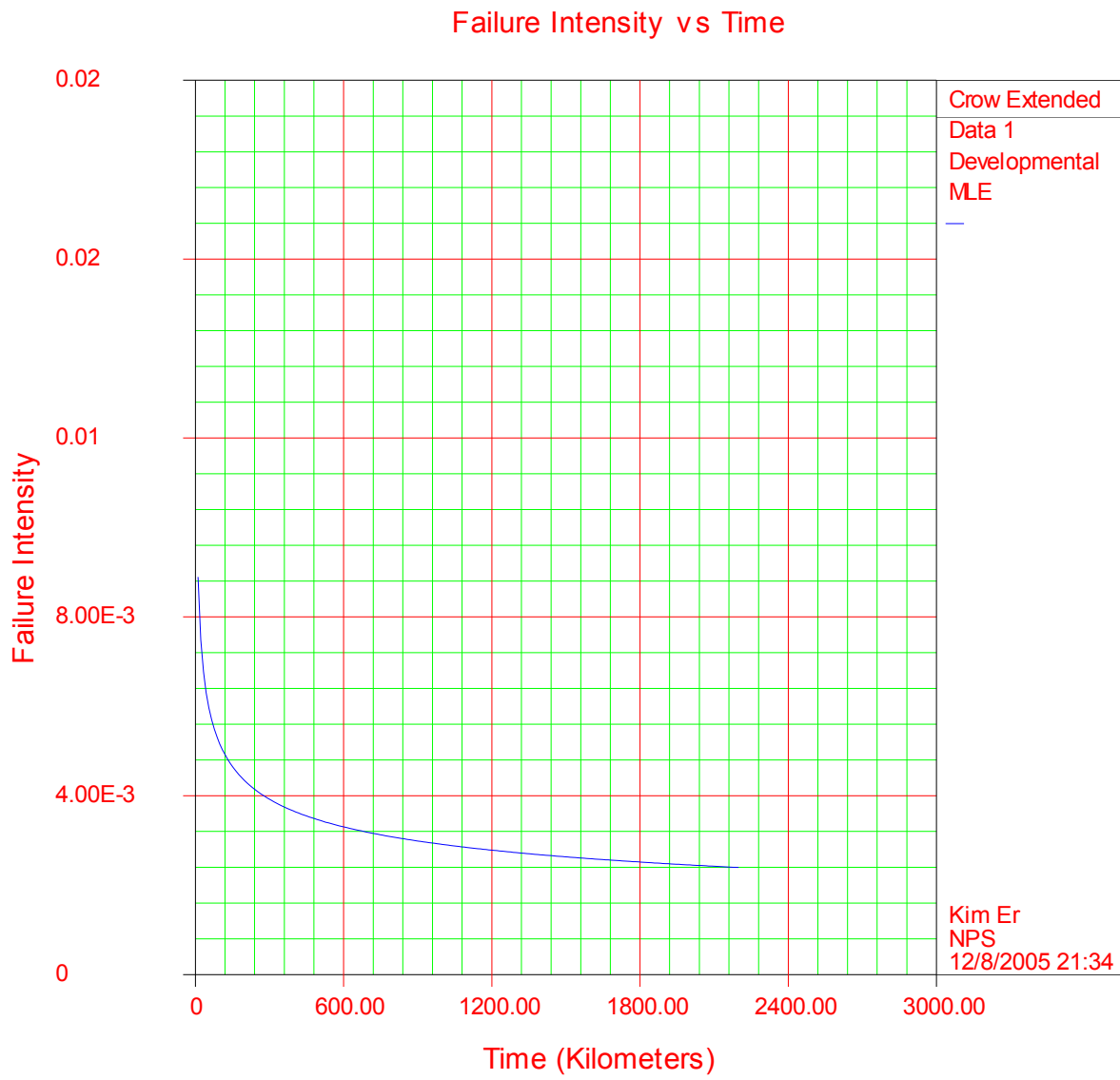


Figure 23. Instantaneous failure intensity vs time plot for Phase 3

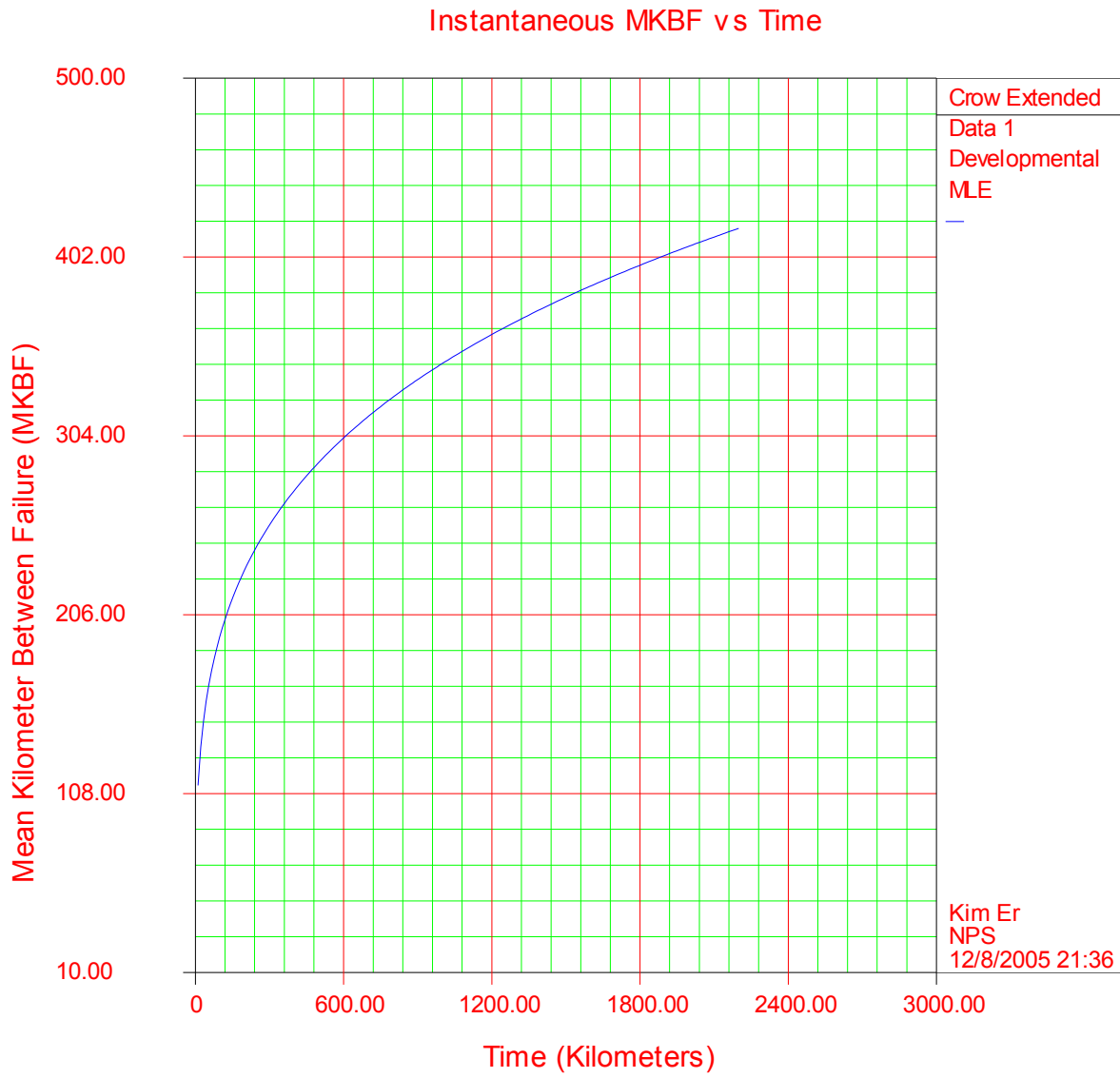


Figure 24. MKBF vs time plot for Phase 3

V. CONCLUSIONS

The key findings of the literature research suggest that the disparity between predicted and field reliability stems from some inherent assumptions of the MIL-HDBK-217 prediction model. First, the constant failure rate assumption that has been generally applied in reliability prediction is not always applicable. However, Drenick's theorem has proven that complex repairable systems, under certain constraints, can be well represented by the exponential distribution. The reliability engineer must be able to recognize when the mathematical simplicity of the constant failure rate model can be used without a substantial penalty in prediction accuracy. Secondly, even if the exponential distribution is applicable, the disparity between predicted and field reliability may still exist in new systems because of unexpected failure modes that may arise in the presence of design and quality deficiencies which will prevent the system from reaching the predicted value. One possible solution to reduce the frequency of occurrence of unexpected failures in the field and for the system's reliability to approach the predicted value is to apply RGT during the development phase.

The results of the reliability analysis for the combat system show that the demonstrated system reliability for both subsystems is initially low. For subsystem A the initial MRBF is only 45 % of the final achieved MRBF. For subsystem B the initial MKBF is only 48 % of the final achieved MKBF. However, the reliability for both subsystems improves as testing progresses. Reliability is finally estimated to meet the predicted value as failure modes are discovered and eliminated through the TAAF process. I conclude that the application of RGT during the developmental phase is effective in minimizing the disparity between predicted and field reliability. Systems that bypass development testing will experience low reliability in the field, which is one of the main causes of disparity between predicted and field reliability.

This thesis has successfully demonstrated the detailed application of the Duane Model and the AMSAA Extended Models for the reliability planning and analysis of a combat system. Some of the important lessons learned on the use of the reliability growth models are summarized below.

In reliability growth planning, the total test time required for the RGT program is sensitive to the following parameters: 1) system's initial reliability, 2) initial test time, 3) growth rate. In most practical cases, the total test time is usually fixed due to time and resources available in the development program. The most accurate way of determining the initial system's reliability is to subject the system to pre-development testing and the initial test time must be long enough for at least the first failure to surface.

The use of failure mode designation such as Type BD and BC associated with the AMSAA Extended Growth Models has provided better visibility over the AMSAA Basic Test-Fix-Test Model. It allows generation of many useful metrics such as: 1) initial system reliability at the beginning of the test, 2) the average effectiveness factor of remedying failure modes, 3) fraction of seen and unseen Type BD failure modes, and 4) system failure rate breakdown for individual failure modes. Knowing the failure rate breakdown of individual failure modes in the system is important as it enables easy identification of failure modes with relatively high failure rate. The reliability of subsystem A and B continues to grow during the RGT because of focused efforts in eliminating these major contributors. In addition, the ability of the AMSAA Extended Test-Find-Test Model to estimate the increased in the system's reliability for Type BD failure modes has allowed for a more in depth analysis of the test data. This is especially useful at the end of the RGT program when the demonstrated reliability of the system is below the target and due to resource constraints further testing is not possible. It is therefore important to know if the final system reliability can meet the requirements after incorporating the delay fixes. For subsystem A, the Extended Test-Find-Test Model estimates the increased in MRBF from 186 rounds to 206 rounds due to three distinct delayed fixes with an assumed EF of 0.6 and thus exceeding the MRBF target of 200 rounds. It is also important to note that the final system reliability is sensitive to the assigned value of EF. To prevent over estimation of the system final reliability, a conservative EF should be assigned since the actual effectiveness of the delayed fixes cannot be determined without further testing.

For new systems under development, the use of the AMSAA NHPP model provides a better representation of the system's failure rate than the exponential distribution because the failure rate is varying with time as testing progresses. Once the

system matures through a period of testing and reliability growth has reached a plateau, the system's failure rate will tend towards being well represented by an exponential distribution.

The use of the various reliability charts such as cumulative failures versus time, failure intensity versus time, MRBF/MKBF versus time have also provided management and technical visibility on how the system is performing during the test which is also a major factor that contributes to the success of the RGT program.

THIS PAGE INTENTIONALLY LEFT BLANK

LIST OF REFERENCES

1. MacDiarmid, Preston, R. (1985). Relating Factory and Field Reliability and Maintainability Measures. *Proceedings Annual. Reliability & Maintainability Symposium*. Philadelphia, Pennsylvania: Institute of Electrical & Electronic Engineers (IEEE).
2. Swett, Colonel Ben, H. (1978). Reliability Growth Management. *Reliability Growth Management Testing and Modeling Seminar Proceedings*. Washington, D.C.: Institute of Environmental Sciences.
3. Dellert, Gregg M. (2001). An Analysis of the Impact of Reliability and Maintainability on the Operating and Support (O&S) Costs and Operational Availability (Ao) of the RAH-66 Comanche Helicopter. Monterey, California: Naval Postgraduate School.
4. Hunter Unmanned Aerial Vehicle (UAV) System Reliability Growth Story. (2001). PM TUAV, Redstone Arsenal,
5. Military Handbook (MIL-HDBK-189): Reliability Growth Management. (1981). Washington, D.C.: Department of Defense (DoD).
6. Blanchard, Benjamin S. (2003). Logistics Engineering and Management (Sixth Edition), New Jersey: Pearson Prentice Hall.
7. Wilkins, Dennis, J. (2002). On-Line Reliability Engineering Resources for the Reliability Professional, 'The Bathtub Curve and Product Failure Behaviour Part One-The Bathtub Curve, Infant Mortality and Burn-in, Issue 21. Retrieved July, 2005, from Weibull.com: On-line Reliability Engineering Resources for the Reliability Professional Web site
<http://www.weibull.com/hotwire/issue21/hottopics21.htm>, last assessed October 2005.
8. Modarres, M. (1993). What Every Engineer should Know About Reliability and Risk Analysis, New York: Marcel Dekker, Inc.

9. Military Handbook (MIL-HDBK-217-2): Reliability Prediction of Electronic Equipments. (1995). Washington, D.C: Department of Defense (DoD).
10. Harris, Norman, O'Connor, Patrick D.T. (1984). Reliability Prediction: Improving the Crystal Ball. *Proceedings Annual Reliability & Maintainability Symposium*. San Francisco, California: Institute of Electrical & Electronic Engineers (IEEE), Inc
11. Limitations of the Exponential Distribution for Reliability Analysis. (n.d.). Retrieved July 2005, from ReliaSoft Website:
<http://www.reliasoft.com/newsletter/4q2001/exponential.htm>, last assessed October 2005
12. Lewis, E.E. (1994). Introduction to Reliability Engineering, Second Edition, New York: John Wiley & Sons, Inc.
13. Collins, Michael. (1998). Error Prediction Models and Field Data. Retrieved August 2005, from Carnegie Mellon University Website:
http://www.ece.cmu.edu/~koopman/des_s99/field_data/#concepts, last assessed October 2005.
14. Economou, Manthos. (2004). The Merits and Limitations of Reliability Predictions. *Proceedings Annual Reliability & Maintainability Symposium*. Los Angeles, California: Institute of Electrical & Electronic Engineers (IEEE), Inc.
15. Lynch, Jeffery, B., Phaller, Lawrence J. (1984). Predicted Vs Test MTBF's....Why the Disparity? *Proceedings Annual Reliability & Maintainability Symposium*. San Francisco, California: Institute of Electrical & Electronic Engineers (IEEE), Inc.
16. *Chapter 9: Reliability Growth*. (n.d). Retrieved July 2005, from Defense Technical Information Center (DTIC) Web site:
http://www.dtic.mil/whs/directives/corres/pdf/32351h_0382/chap9.pdf, last assessed November 2005.

17. Reliability Prediction Models: Use and Evaluation. (n.d.). Retrieved August 2005, from Relex Software Web site:
http://www.relexsoftware.com/resources/art/art_predmodels2.asp, last assessed October 2005.
18. Murphy, Kenneth E., Charles M. Carter & Steven O. Brown. (2002). The Exponential Distribution: the Good, the Bad and the Ugly. A Practical Guide to its Implementation. *Proceedings Annual Reliability & Maintainability Symposium*. Seattle, Washington: Institute of Electrical & Electronic Engineers (IEEE), Inc.
19. On-Line Reliability Engineering Resources for the Reliability Professional. (2005). Retrieved September 2005, from Weibull.com: On-line Reliability Engineering Resources for the Reliability Professional Web site:
http://www.weibull.com/RelGrowthWeb/Goodness-of-Fit_Tests_for_the_Crow-AMSAA_Model.htm, last assessed November 2005.
20. Crow, Larry H. (2004). *An Extended Reliability Growth Model for Managing And Assessing Corrective Actions. Annual Reliability & Maintainability Symposium*. Los Angeles, California: Institute of Electrical & Electronic Engineers (IEEE), Inc.
21. ReliaSoft's RGA Software for Repairable Systems and Reliability Growth Analysis. (n.d.). Retrieved October 2005, from ReliaSoft Web site:
<http://www.reliasoft.com/RG/features.htm>, last assessed November 2005.
22. NIST/SEMATECH e-Handbook of Statistical Methods. (n.d.). Retrieved November 2005, from NIST/SEMATECH Web site:
<http://www.itl.nist.gov/div898/handbook/index.htm>, last assessed November 2005.

THIS PAGE INTENTIONALLY LEFT BLANK

INITIAL DISTRIBUTION LIST

1. Defense Technical Information Center
Ft. Belvoir, Virginia
2. Dr. David H. Olwell
Naval Postgraduate School
Monterey, California
3. Morris R. Driels
Naval Postgraduate School
Monterey, California
4. Mr Pantelis Vassiliou
ReliaSoft, IN.
Tucson, Arizona
5. Defence Science & Technology Agency (DSTA)
Singapore